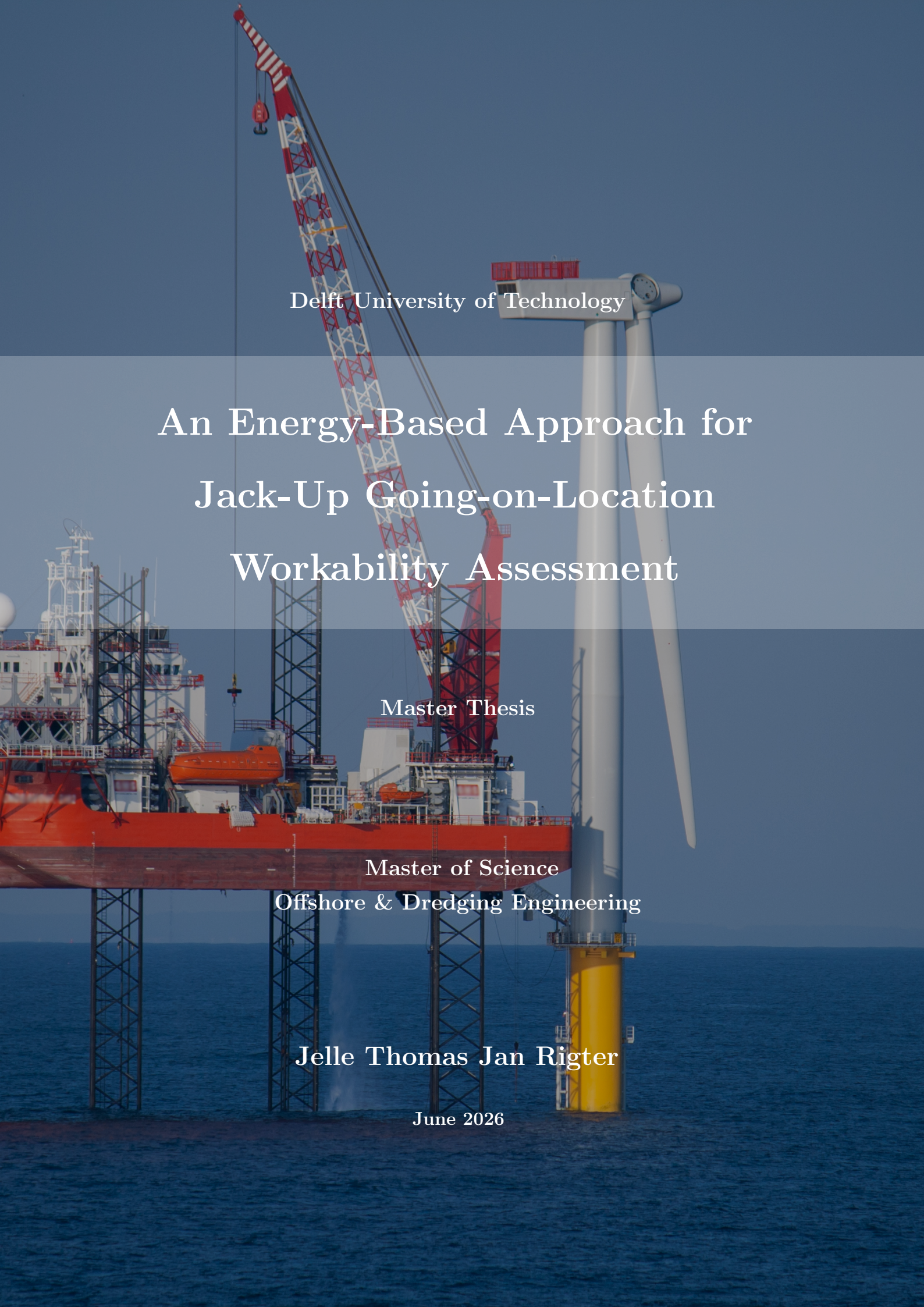

Delft University of Technology

An Energy-Based Approach for Jack-Up Going-on-Location Workability Assessment

Master Thesis

Master of Science
Offshore & Dredging Engineering

Jelle Thomas Jan Rigter

June 2026

MASTER THESIS

An Energy-Based Approach for Jack-Up Going-on-Location Workability Assessment

by

Jelle Rigter

Offshore and Dredging Engineering

Jelle Rigter - 4885082

Supervisor: Dr. Ir. J.S. Hoving
Daily Supervisor: Ir. G. Holland
Chairman: Prof.dr. A.V. Metrikine
Supervisor: Ir. M. Hoogeveen

AI usage statement

During the preparation of this thesis, artificial intelligence tools were used to support the writing and visualisation process. ChatGPT was used to assist with formulation, wording, and improving the clarity of written text. The scientific content, analysis, methodology, results, and conclusions remain the author's own work.

Gemini was used to generate images included in the thesis. Any AI-generated visual material was reviewed and selected by the author to ensure that it was appropriate and consistent with the content of the thesis.

Abstract

Going-on-Location (GoL) is a critical phase in jack-up vessel operations, during which the unit transitions from a free-floating condition to seabed support. During touchdown, the spudcans may experience short-duration, high-magnitude impact forces due to the coupled effects of wave-induced vessel motions, nonlinear soil-spudcan contact, and leg deformation. Current GoL workability assessments rely on detailed time-domain simulations to determine impact forces, structural unity checks, and allowable sea states. Although these methods provide a physics-based basis for operational decision-making, they are computationally demanding and mainly describe simulation outcomes rather than the underlying relation between vessel motion and touchdown severity.

This thesis investigates whether the global mechanical energy response of a jack-up vessel can be used as a physically interpretable indicator for touchdown severity and GoL workability assessment. An energy formulation is developed within an existing time-domain GoL simulation framework and verified using energy and power balance relations. The method is applied to transient impact simulations with seabed contact enabled and to free-floating steady-state simulations in which seabed contact is disabled.

The results show that global mechanical energy provides useful physical interpretation, but does not directly predict impact severity. Critical wave realisations do not exhibit a consistent pre-impact energy level, energy build-up, or common energy peak. Instead, elevated periods in the free-floating global mechanical energy response are most relevant when they occur within the same time window as the touchdown interval identified in the corresponding impact simulation. Three-hour free-floating simulations can characterise the timing, magnitude, and persistence of these elevated energy periods, but do not provide a consistent threshold between allowable and non-allowable GoL cases.

It is concluded that global mechanical energy should not be used as a standalone workability criterion. Its main value lies in identifying potentially critical response periods and interpreting touchdown behaviour relative to seabed contact. Future work should focus on near-touchdown and initial-contact simulations to relate energy transfer more directly to impact magnitude, while RAO-based reconstruction of the free-floating energy response could be investigated as an efficient screening method.

Preface

With this thesis, my time as a student comes to an end. Looking back, I feel grateful for the valuable and enjoyable years that have shaped me, both academically and personally. My student years have been full of learning, growth, new experiences, and memorable moments, and I am happy to close this chapter with the completion of this thesis.

Working on this topic has been a very enjoyable experience. It gave me the opportunity to dive deeper into a complex engineering problem and to better understand how different parts of engineering come together in practice. A jack-up vessel combines many different technical disciplines, which made the subject both challenging and interesting. Learning how these principles interact during a real offshore operation has strengthened my interest in engineering and its practical relevance.

This thesis would not have been possible without the support and guidance of my supervisory team. First, I would like to thank Gijs, my daily supervisor, for his continuous involvement throughout the project. Our discussions, his constructive feedback, and his help in structuring my thoughts have been very valuable in shaping both the research process and the final thesis.

I am also very grateful to Maas for his supervision and critical input during the project. His experience and perspective helped me define the scope of the research, keep the work focused, and ensure that the project remained relevant from both a technical and practical point of view.

Furthermore, I would like to thank Jeroen for his guidance from the university side and for his feedback, which helped me think more critically about the direction and communication of the research. Finally, I would like to thank Andrei for sharing his technical knowledge, for explaining difficult principles in a clear and understandable way, and for helping me better understand and interpret my results.

Together, their guidance, feedback, and different perspectives have been very important throughout this thesis. They made the process not only educational, but also enjoyable.

Jelle Rigter
Rotterdam, June 2026

Contents

List of Figures

Nomenclature

Symbol	Description
$A(\omega)$	Frequency-dependent added-mass matrix [kg, kg m, kg m^2]
A_{eq}	Equivalent added-mass matrix [kg, kg m, kg m^2]
$C(\omega)$	Frequency-dependent radiation-damping matrix [Ns/m, Nms/rad]
C_{eq}	Equivalent radiation-damping matrix [Ns/m, Nms/rad]
E_{ff}	Mechanical energy in the free-floating configuration [J]
E_{imp}	Mechanical energy in the impact configuration [J]
E_{kin}	Kinetic energy [J]
E_{pot}	Potential energy [J]
E_{strain}	Strain energy stored in the legs [J]
E_{tot}	Total mechanical energy [J]
F_{exc}	Wave-excitation force vector [N, Nm]
F_{imp}	Impact-force vector due to spudcan–seabed contact [N, Nm]
H_s	Significant wave height [m]
K	Hydrostatic stiffness matrix [N/m, Nm/rad]
K_{mooring}	Equivalent mooring or positioning stiffness matrix [N/m, Nm/rad]
M	Mass matrix [kg, kg m, kg m^2]
M_{LH}	Bending moment at the leg–hull interface [Nm]
$N_{1/3}$	Number of highest peaks used for the one-third highest response measure [-]
P_{in}	Incoming power [W]
P_{diss}	Dissipated power [W]
RAO_{load}	Load response-amplitude operator [N/m, Nm/m]
RAO_{q_j}	Motion response-amplitude operator for degree of freedom j [m/m, rad/m]
R	Rotation matrix from local to global reference frame [-]
r	Position vector from local reference point to centre of gravity [m]
$[r]_\times$	Skew-symmetric matrix associated with r [m]
$S_\zeta(\omega)$	Wave spectrum [m^{2}s]
$S_{\zeta,N}(\omega)$	Normalised wave spectrum [s]
T	Adjoint transformation matrix [-]
T_p	Peak wave period [s]
β	Wave direction relative to vessel heading [°]
γ	JONSWAP peakedness factor [-]
η	Wave elevation [m]

Abbreviation	**Meaning**
BEM	Boundary Element Method
COG	Centre of Gravity
DNV	Det Norske Veritas
DOF	Degree of Freedom
DP	Dynamic Positioning
DSV	Downward Spudcan Velocity
GoL	Going-on-Location
JONSWAP	Joint North Sea Wave Project spectrum
MOM	Marine Operations Manual
MWL	Mean Water Level
P90	90th percentile response value
RAO	Response-Amplitude Operator
UC	Unity Check
WTIV	Wind Turbine Installation Vessel

Introduction 1

The global demand for renewable energy has increased rapidly in response to climate targets and international policy commitments. Many countries have introduced long-term strategies to reduce greenhouse gas emissions and expand the share of renewable energy in the power system. Within the European Union, the European Green Deal aims to achieve climate neutrality by 2050, with intermediate targets promoting a substantial expansion of renewable electricity production (European Commission, 2024).

Wind energy plays a central role in this transition due to its large-scale generation potential and increasing technological maturity. In recent years, wind power production in Europe has grown significantly and has begun to replace electricity generation from fossil fuel sources. This development is particularly visible in the rapid expansion of offshore wind farms, which benefit from favourable wind conditions and enable large-scale electricity generation (Green, 2024).

The installation and maintenance of offshore wind farms rely heavily on specialised offshore vessels. Among these, jack-up vessels play a crucial role by providing a stable offshore platform that allows heavy lifting operations, such as the installation of turbine foundations, towers and nacelles, to be performed safely under marine conditions (Identec Solutions, 2024).

Figure 1.1: Jack-up vessel in elevated condition during offshore wind turbine installation (SWZ Maritime, 2022)

1.1 The Going-on-Location operation of a jack-up

A jack-up vessel is a self-elevating mobile offshore structure: it can raise itself above the sea surface by means of its own jacking system, transforming from a floating vessel into a stable offshore platform. It typically consists of three primary components: a hull, movable legs and a jacking system. Jack-ups are flexible in use and offer mobile operability, which makes an offshore operation very cost effective.

The hull is the main body of the jack-up. It is a watertight structure that contains the accommodation areas, machinery, equipment, and operational facilities. The hull is connected through three or more steel legs. These are large steel structures that can be raised or lowered using the jacking system. Upon arrival at a location, the legs are lowered until they reach the seabed. The hull is subsequently jacked upward along the legs until it is positioned safely above the water level, clear of waves. Most jack-up units are fitted with spudcans at the base of each leg. A spudcan is a large steel footing designed to increase the contact area between the leg and the seabed. Typically rounded or conical in shape, spudcans allow controlled penetration into the soil and help establish a stable foundation for the elevated unit (Vazquez et al., 2005).

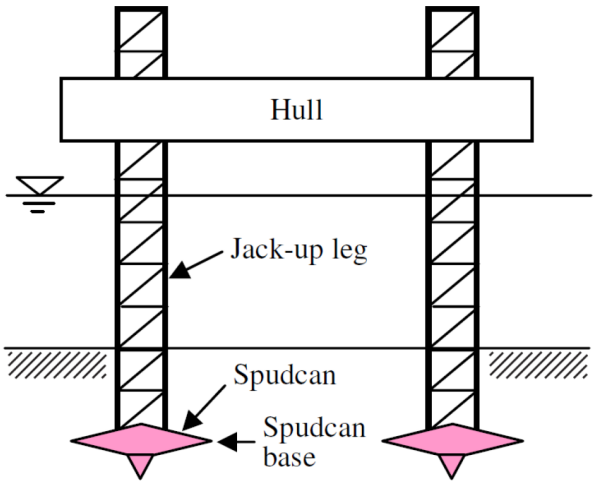

Figure 1.2: Schematic representation of the main structural components of a jack-up unit, adapted from (Lee & Randolph, 2010)

The transition from a floating condition to an elevated condition of a jack-up is referred to as Going-on-Location (GoL). During this operation, the unit is positioned at the intended site while the legs are lowered toward the seabed. The process starts in a free-floating phase (I), where hull motions are governed primarily by wave loading. This is followed by the impact phase (II), during which the spudcans make first contact with the seabed and intermittent impacts may occur while the hull continues to move under wave action. Finally, in the lifting phase (III), continuous seabed contact is established and the hull is gradually elevated, transferring structural support from buoyancy to the seabed through the legs and spudcans.

The impact phase is considered the most critical part of this procedure. When the legs are close to the seabed, the hull still experiences wave-induced motions and the spudcans may impact the seabed. This contact leads to short-duration and potentially high impact loads. These loads often determine both the structural limits and the operational workability limits of the jack-up during installation.

1.2 Problem statement and objective

The short-duration, high impact loads during the impact phase cannot be described by a single constant force or deterministic touchdown condition. Detailed time-domain simulations are therefore commonly used to capture the transient and nonlinear behaviour of the system. Also, since an irregular sea state does not correspond to a unique wave time series, several random wave realisations or seeds may be required for the same environmental condition. This becomes computationally demanding when many environmental conditions must be evaluated. In addition, response quantities such as contact forces, bending moments and unity checks mainly describe the severity of individual simulations, but do not directly provide a physically interpretable relation between pre-impact vessel motion and structural response.

This motivates the investigation of an indicator for touchdown severity and GoL workability. The objective of this thesis is to investigate whether the global mechanical energy of a jack-up vessel can be used as a physically interpretable indicator for impact severity during the GoL operation, and whether the free-floating energy response contains information that can support preliminary screening of allowable cases before full touchdown simulations are performed.

1.2.1 Research questions

The main research question is defined as:

> *To what extent can the global mechanical energy response of a jack-up vessel be used as a physically interpretable indicator for touchdown severity and GoL workability assessment?*

This main question is supported by two sub-questions:

1. *To what extent can the time-dependent energy response during the impact phase be used as an indicator for transient touchdown severity?*
2. *To what extent can steady-state free-floating energy quantities provide an indication of allowable and non-allowable GoL cases?*

The first sub-question addresses the interpretation of the behaviour during impact, while the second sub-question investigates whether pre-impact energy quantities may support the early identification of allowable cases.

In this thesis, GoL workability is defined as the ability to perform a jack-up GoL operation safely under given environmental conditions without exceeding predefined structural or operational limits. A case is considered allowable when the simulated response remains below the relevant capacity limits, typically expressed by unity checks below 1.0. Workability limits therefore define the boundary between allowable and non-allowable sea states, expressed by combinations of wave height, wave period and wave direction.

1.3 Research methodology

The methodology consists of a modelling framework in which the GoL operation is divided into a free-floating simulation and an impact simulation. The vessel response is described using an existing time-domain GoL simulation framework, which represents the coupled hydrodynamic,

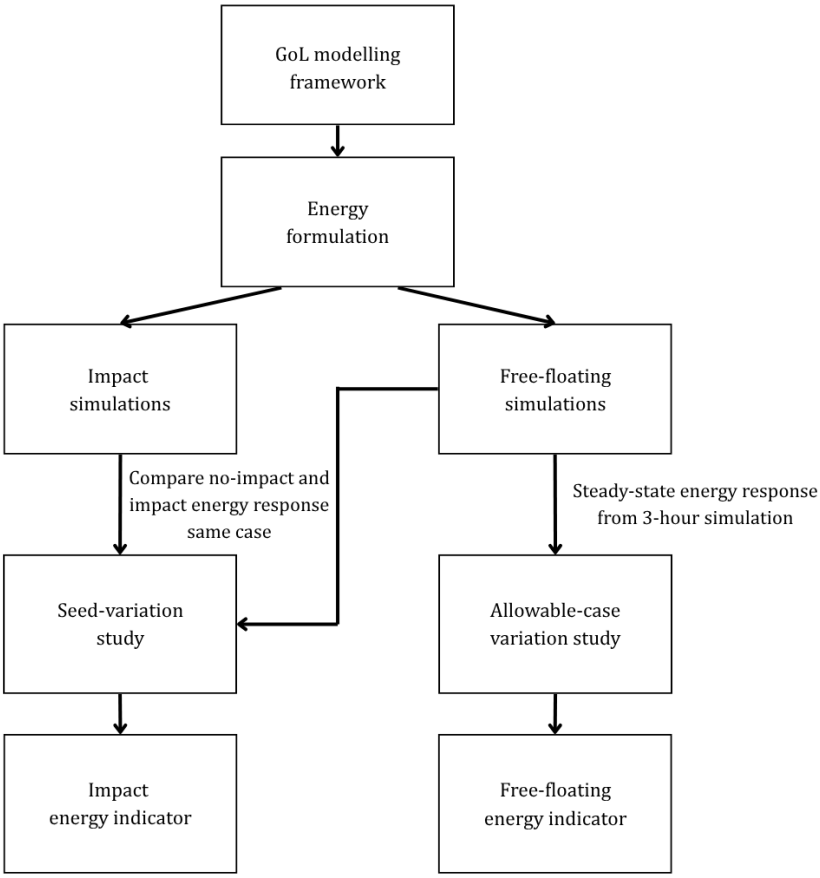

Figure 1.3: Overview of the research methodology used to evaluate energy-based indicators from free-floating steady-state simulations and impact simulations

structural and soil-spudcan response of the jack-up during the operation. Within this framework, an energy formulation is developed and verified using energy and power balance relations. This provides a consistent basis for evaluating the kinetic and potential energy associated with the global vessel motion.

The energy formulation is then applied to two complementary simulation approaches. First, impact simulations are performed with seabed contact enabled. These time-domain simulations capture the transient vessel response, seabed contact forces and structural load transfer during touchdown. For this simulation, the energy formulation is expanded to include contact work, leg deformation and soil-spudcan interaction. Touchdown is therefore interpreted as a time-dependent energy-transfer process rather than as a single peak-load event.

Second, free-floating simulations are performed by disabling seabed contact. These simulations are used to evaluate the energy response of the jack-up before touchdown occurs. For the allowable-case variation study, three-hour free-floating simulations are used to extract steady-state energy quantities of different allowable cases. In addition, the same no-impact approach is used for the wave seeds considered in the impact study, allowing the free-floating energy response to be compared with the corresponding impact response for the same wave realisation.

The two simulation approaches are used to investigate whether energy-based quantities can be identified that are relevant for GoL workability assessment. The free-floating steady-state

simulations are used to explore whether pre-impact energy behaviour contains information about allowable or critical GoL conditions, while the impact simulations are used to investigate whether time-dependent energy quantities during touchdown relate to transient impact severity.

1.4 Research gap and novelty

Over the years GoL assessment methods have evolved from simple limiting wave-height criteria towards advanced simulation-based approaches that account for vessel motions, structural response, seabed interaction and site-specific environmental conditions. Modern time-domain models are able to represent the GoL process with a high degree of physical realism and are commonly used to determine operational limits through calculated impact loads, structural response quantities and unity checks. These methods therefore provide a detailed basis for assessing whether a given GoL condition is allowable. However, these assessments must be repeated across a wide range of environmental conditions during a full location assessment, causing the computational effort required to become significant.

Energy-based approaches have been introduced in GoL assessment as a means of estimating impact severity without relying solely on full time-domain simulations. However, these methods generally rely on simplified assumptions, such as idealised energy transfer, simplified contact behaviour or reduced representations of vessel dynamics. Consequently, they often result in conservative workability assessments and remain limited in their ability to capture touchdown severity. The gap therefore lies between simplified energy-based methods and high-fidelity time-domain simulations.

The novelty of this thesis lies in the development and evaluation of an energy-based perspective at the same level of detail as current state-of-practice industrial GoL simulations. The study aims to bridge the gap between simplified energy-based assessment methods and detailed time-domain simulations, while exploring the potential of energy-based quantities to support reduced indicators for GoL workability assessment.

Impact loads, unity checks and allowable sea-state criteria remain necessary for operational decision-making. However, if robust energy-based indicators can be identified, they may provide an additional layer of physical interpretation and support faster preliminary screening of GoL conditions, thereby reducing the reliance on computationally expensive time-domain simulations for every assessed case.

State of the art 2

This chapter reviews GoL workability assessment from three complementary perspectives. First, the physical interpretation of GoL is introduced to show that its assessment cannot be reduced to a single environmental limit. Second, academic and industrial assessment methods are reviewed to show how the field has progressively moved toward site-specific simulation-based approaches. Third, energy-based interpretations are discussed to identify whether energy can provide an additional physically interpretable indicator for touchdown severity and pre-impact workability.

2.1 Going-on-location as a workability assessment problem

Going-on-location assessment is concerned with determining whether the transition from a floating condition to seabed support can be performed safely under forecasted environmental conditions. Within the GoL sequence, the impact phase is often considered critical, as the initial contact between the spudcans and seabed can generate large short-duration impact loads in the legs, spudcans, and jacking system.

2.1.1 Phases of the GoL operation

The GoL process consists of three phases, which are explained in this section. The overall process is visualized in Figure 2.1.

- **Free-floating phase (I):** The GoL process starts when the jack-up arrives at the intended location in a floating condition. During this stage, the vessel is typically maintained on position by towing vessels or a dynamic positioning (DP) system while the legs are lowered towards the seabed and the hull remains exposed to wave-induced motions (Journée & Massie, 2008). The system response is therefore mainly governed by hydrodynamic loading, while the spudcans move together with the hull and legs.
- **Impact phase (II):** During this phase, the legs are lowered until one or more spudcans come into contact with the seabed while the hull is still moving under wave excitation. The contact may be intermittent, because the vessel can continue to move vertically and rotationally under wave excitation. As a result, the spudcan can touch the seabed, lose contact and touch down again before continuous support is established. This phase is critical because the mechanical boundary condition at the spudcan changes rapidly from free motion in the water column to constrained interaction with the seabed. Once contact occurs, the soil resists the spudcan motion and introduces reaction forces that are transferred into the legs, jacking system, and hull. Since this transition occurs over a short time interval while the hull is still moving under wave excitation, significant impact loads can develop.
- **Lifting phase (III):** After sufficient penetration and contact development, the jack-up enters a soft-pinned condition. In this phase, the spudcans remain in contact with the seabed and the vessel motions are increasingly restricted by soil resistance. The response

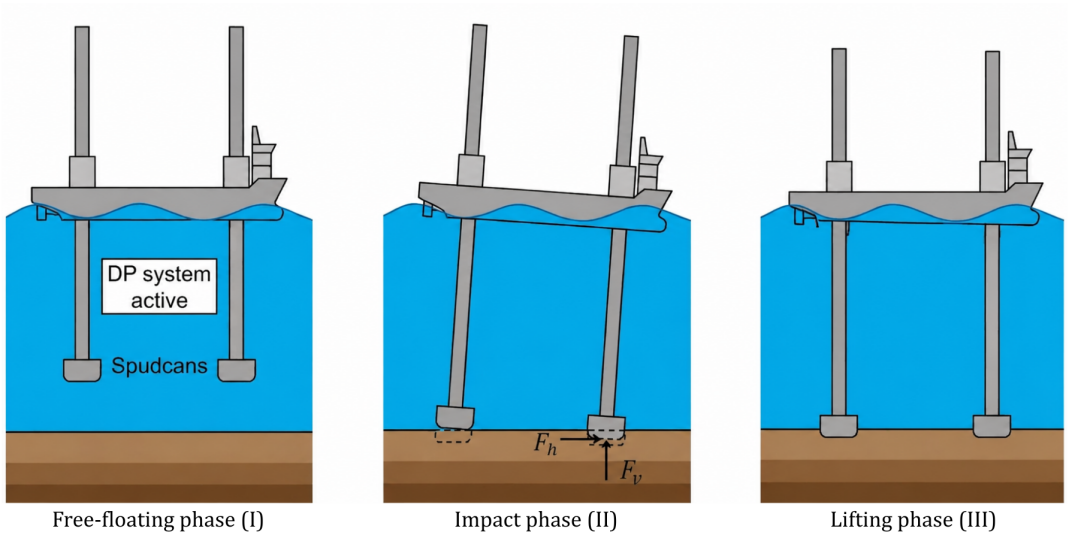

Figure 2.1: Three phases of a jack-up Going-on-Location

is no longer governed only by floating hydrodynamics, but by the coupled behaviour of the hull, legs and seabed.

This sequence, from a hydrodynamically dominated floating condition towards a seabed-supported response through a transient impact stage, is acknowledged in several previous studies on jack-up installation dynamics and operational assessment (Chakrabarti, 2012; Daun & Olsson, 2014; Matter et al., 2005; Ringsberg et al., 2017; Smith et al., 1994, 1995).

2.1.2 Impact behaviour during touchdown

Jack-ups are flexible structural systems in which loads are transferred through the spudcan, legs, jacking system and hull. Studies on nonlinear jack-up response show that the global behaviour may be influenced by hydrodynamic loading, second-order structural effects, soil-structure interaction, deck-leg interaction and dynamic amplification (Spidsoe & Karunakaran, 1996; Williams et al., 1998). These studies mainly consider jack-ups in elevated condition, however their conclusions are relevant for GoL assessment because impact loads are also transmitted through the legs and may excite the global structural system. This supports the view that GoL touchdown should be treated as a coupled transient response of the complete jack-up system.

The impact response is difficult to predict because several nonlinear and time-dependent mechanisms interact (Chakrabarti, 2012). First, the response is transient: contact forces, vessel motions, leg deformation, and soil reaction may change rapidly during the short contact interval, making the impact dependent on the instantaneous position and velocity of the jack-up at seabed contact (Vazquez et al., 2016). Second, the pre-impact vessel motion is governed by irregular wave excitation. A sea state defines statistical wave properties, but not one unique time signal, meaning that different wave realisations may lead to different combinations of heave, roll, and pitch at touchdown (Chakrabarti, 2012; Guachamin Acero et al., 2016). Third, the spudcan-soil interaction is nonlinear. During first contact, a spudcan may touch down, unload, or partially lose contact before stable support is established, while plastic soil deformation makes the soil reaction dependent on penetration depth and loading history (Holland & Hoogeveen, 2023). Finally, the jack-up legs are flexible structural members that bend under contact loads and store part of the impact energy as strain energy, thereby affecting the load transfer between

hull, legs, spudcans, and seabed (Chakrabarti, 2012).

From an impact-mechanics perspective, touchdown can be interpreted as a short-duration event in which the relative velocity between the spudcan and seabed is reduced through contact forces. Classical impact theory describes such events as involving large forces acting over short time intervals, during which the velocities, contact conditions and internal stress states of the interacting bodies change rapidly (Goldsmith, 1960). Goldsmith further emphasizes that impact problems are inherently complex because inertia effects, structural deformation, contact interaction and energy transfer occur simultaneously and are strongly coupled during the collision process (Goldsmith, 1960).

2.2 Academic approaches to GoL assessment

This section reviews how academic GoL assessment developed from simplified operational limits towards response-based and site-specific methods. Early studies linked allowable operations to vessel motions and touchdown velocities, while later work increasingly incorporated hydrodynamic response, structural flexibility and soil-spudcan interaction. Together, these studies show that GoL impact assessment must be understood as a coupled hydrodynamic, structural and geotechnical response problem.

2.2.1 Early operational limits and risk-based assessment

Early GoL assessment was primarily concerned with defining whether touchdown could be performed without exceeding acceptable leg loads. In practice, this was often reduced to simple environmental limits, such as a maximum significant wave height H_s, typically 5 ft ($\approx 1.5\,\mathrm{m}$) (Smith et al., 1994).

Miller et al. (1993) showed that such limits are insufficient, because jack-up motions change as the legs are lowered; for certain leg lengths and wave periods, pitch and roll motions increase and govern the impact velocity. Building on this motion-response perspective, Matter et al. (2005) related allowable impact forces to roll and pitch amplitudes, and converted these response limits into allowable wave-height and wave-period curves. These studies shifted GoL assessment from fixed environmental thresholds to response-based operational limits.

In parallel, Smith et al. (1994) developed limiting responses that relate vessel motions, touchdown velocities and allowable leg loads, introducing a more probabilistic workability framework. Building on this approach, Smith et al. (1995) developed limiting response curves that directly relate hydrodynamic response characteristics and touchdown velocities to go/no-go operational criteria. These curves define allowable combinations of vessel motions under varying environmental conditions. Figure 2.2 illustrates an example of such a limiting vertical touchdown velocity curve. The dashed line at 67.5° illustrates one example wave heading, where the intersection with the curve determines the maximum allowable touchdown velocity for that particular approach angle.

Overall, these studies established the shift from fixed environmental criteria to response-based GoL assessment, where limits are derived from vessel motions, impact response and structural capacity. However, they still mainly defined generalised limits, motivating later site-specific and weather-window-based approaches.

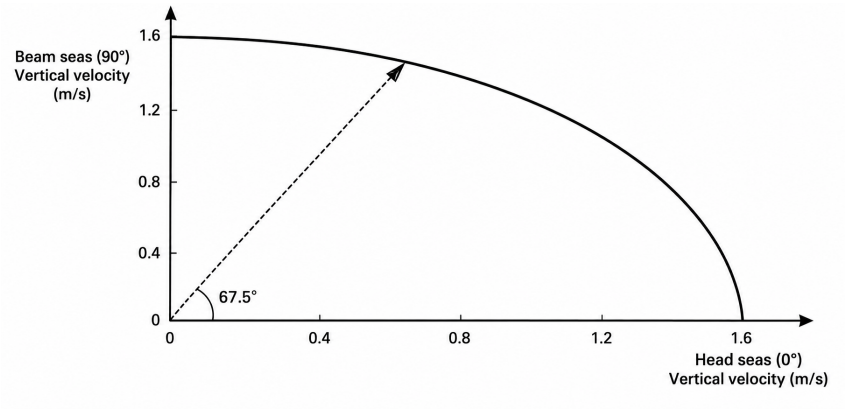

Figure 2.2: Limiting vertical velocity curve for touchdown on dense sand under oblique (67.5°) sea conditions. Adapted from Smith et al. (1995), figure redrawn for improved readability.

2.2.2 Site-specific and weather-window assessment

Building on these response-based methods, later research focused on the site-specific nature of GoL impact assessment. These studies showed that impact force depends not only on general response limits, but on the actual combination of vessel behaviour, water depth, wave period, wave direction, soil condition and structural capacity.

Chakrabarti (2012) presented a site-specific GoL approach in which touchdown was treated as a coupled hydrodynamic, geotechnical and structural interaction. The study considered the rigid-body motions of the floating jack-up, the nonlinear resistance of the seabed, the elastic dynamic response of the leg, and the structural strength of the jack-up. This work showed that touchdown severity depends on how impact energy is absorbed by soil deformation and leg vibration. However, the method still used simplified soil and structural representations, limiting how well local seabed conditions and structural response could be represented.

This limitation was partly addressed by Daun and Olsson (2014) and Ringsberg et al. (2017), who further developed site-specific and response-based methodologies. Their studies combined hydrodynamic motion analysis, nonlinear soil-structure interaction and structural response calculations to predict impact forces and compare them with structural criteria or capacity limits. Through this approach, site-specific impact simulations are translated into practical operability and weather-window criteria. Nevertheless, these approaches still retained simplifications, including idealised seabed conditions, limited soil load history and structural evaluation partly separated from the impact simulation.

2.2.3 Soil-spudcan interaction and seabed deformation

Soil-spudcan interaction is important in GoL impact assessment because the seabed controls how the incoming vessel motion is converted into contact loads during touchdown. The soil can deform, yield and dissipate part of the incoming energy, which influences the contact duration, peak impact force and load transfer into the jack-up leg.

Previous studies show that this interaction cannot be represented adequately by a simple rigid or static boundary condition. Foundation response depends on penetration depth, loading path, combined loading and soil layering Cassidy and Houlsby (1999), Fang et al. (2019), and Hu et al. (2021). These effects are relevant for GoL because touchdown involves not only penetration, but

also dynamic contact between the spudcan and seabed. Le et al. (2021) showed that collision angle and soil properties strongly influence the resulting impact force during leg lowering.

The importance of seabed deformability is further demonstrated by Vazquez et al. (2017), who showed that deformable seabed models can produce lower vertical and horizontal reactions than stiff non-deforming seabed models due to plastic soil deformation during touchdown. Conversely, Izadi and Vazquez (2023) showed that very stiff or hard seabeds can lead to high dynamic shock loads because the momentum exchange occurs over a shorter contact duration with limited deformation.

Together, these studies show that soil-spudcan interaction is a major source of complexity in GoL impact assessment. Soil behaviour is therefore recognised as one of the mechanisms that makes the GoL response strongly nonlinear and difficult to simplify, and that should be represented sufficiently well in the coupled assessment framework.

2.3 State of practice in industry

Academic studies mainly help to understand the physical mechanisms that govern touchdown during GoL. In industrial practice, this understanding must be translated into operational limits, weather windows and go/no-go decisions. Different assessment methods are used for this purpose, ranging from simplified guideline-based approaches to detailed site-specific time-domain simulations.

2.3.1 Conservative guideline-based practice

In industrial practice, the operational limits for jack-up units are commonly formalised in vessel-specific marine operation documentation, such as the Marine Operations Manual (MOM). This manual describes the unit design, operational procedures and limiting environmental conditions under which the jack-up may safely operate. For GoL operations, these limits are commonly derived in accordance with recognised offshore guidelines, such as DNV recommended practices for self-elevating units (DNV, 2022).

The DNV guideline states that limiting environmental conditions, such as waves, current, wind and vessel motions, should be specified by the designer. In practice, these limits form part of the operational envelope of the unit and are typically included in the MOM. For a simplified bottom impact assessment, DNV assumes that the impact force is governed by roll or pitch motion of the self-elevating unit. The rotational energy associated with this motion is assumed to be absorbed by the impacted leg and the supporting structure in the hull. The simplified method is based on the following conservative assumptions:

1. only one leg touches the bottom;
2. the lower end of the leg is stopped immediately when the leg touches the bottom;
3. the seabed is assumed to be infinitely rigid.

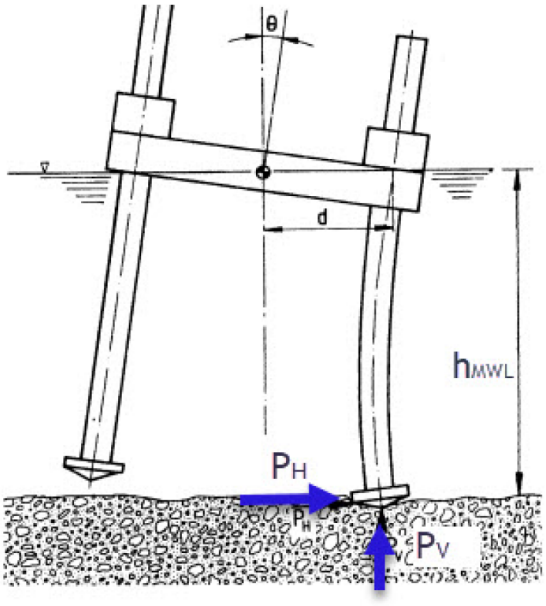

Figure 2.3: Bottom impact on jack-up legs, adapted from DNV-RP-C104 (DNV, 2022).

Under these assumptions, the horizontal and vertical impact force components may be calculated as follows:

$$P_H = \frac{2\pi\theta}{T}\sqrt{\frac{I_m k_H}{1+\frac{k_V}{k_H}\left(\frac{d}{h_{\mathrm{MWL}}}\right)^2}}$$

$$P_V = \frac{2\pi\theta}{T}\sqrt{\frac{I_m k_V}{1+\frac{k_H}{k_V}\left(\frac{h_{\mathrm{MWL}}}{d}\right)^2}}$$

where P_H is the horizontal impact force component, P_V is the vertical impact force component, k_H is the overall lateral stiffness of the leg, and k_V is the overall vertical stiffness of the leg including vertical fixation at the hull. Furthermore, I_m is the mass moment of inertia, T is the period, and θ is the corresponding amplitude. These measures are all only with respect to roll and pitch. The parameters d and h_{MWL} describe the geometric relation between the impacted leg, the hull motion and the mean water level, as illustrated in Figure 2.3.

The simplified formulation provided in DNV-RP-C104 offers a practical and conservative basis for defining operational limits during GoL. However, the assumptions simplify the actual process considerably which makes the resulting operational limits conservative and may underestimate the workability that is actually achievable offshore.

2.3.2 Site-specific GoL assessment framework in industry

Site-specific assessment methods are increasingly used to determine operational limits for GoL operations. Holland and Hoogeveen (2023) present a framework in which the jack-up response is simulated using three main components: a hydrodynamic model, a structural model, and a soil-spudcan interaction model. These components are coupled through a multi-body representation

of the jack-up, in which the hull and spudcans are treated as separate bodies governed by their own equations of motion (Figure 2.4a).

The hydrodynamic model describes the wave-induced loading and vessel motions, while the structural model represents the stiffness and load transfer within the jack-up structure. The most important aspect of the framework is the soil-spudcan interaction model, which includes elasto-plastic soil behaviour. Unlike simplified rigid seabed assumptions, the soil response depends not only on the instantaneous spudcan displacement, but also on the loading history. This introduces memory effects through permanent plastic deformation, hysteresis and damping during repeated penetration and unloading cycles.

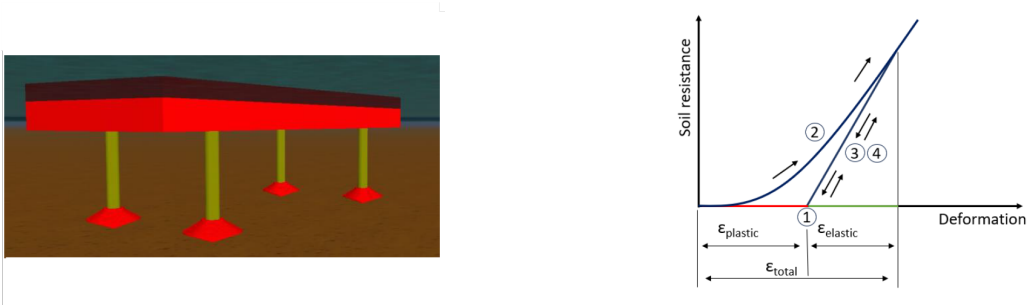

(a) Graphical representation of GoL framework.

(b) Schematic soil resistance–deformation relation for elasto-plastic soil–spudcan interaction.

Figure 2.4: GoL modelling framework and soil–spudcan interaction model (Holland & Hoogeveen, 2023).

Figure 2.4b schematically illustrates the elasto-plastic character of the soil–spudcan interaction. During initial penetration, the soil resistance follows a virgin loading path (2). When the spudcan unloads (3), only part of the deformation is recovered elastically (1), while the remaining deformation is permanent. During subsequent reloading (4), the soil response therefore depends on the previous loading history. This behaviour is important for GoL simulations, because the spudcan may repeatedly touch down, unload and reload before a stable soft-pinned condition is reached.

2.3.3 Workability limits and operational decision-making

Workability assessment is used during project planning to estimate the expected operability, to identify suitable weather windows, and to evaluate potential downtime caused by unfavourable environmental conditions (Guachamin Acero et al., 2016).

Figure 2.5 illustrates how the current GoL assessment process converts model response into an operational decision. The calculated responses by the framework are compared with the allowable structural capacity of the jack-up. The comparison is commonly expressed by a Unity Check (UC), defined as the ratio between the calculated response and the corresponding allowable capacity. A UC value smaller than 1 indicates that the capacity is not exceeded, while a value larger than 1 indicates that the operational limit has been surpassed.

The resulting workability limits are usually provided as tables that specify the maximum allowable H_s for combinations of T_p and wave direction. Here, H_s represents the characteristic wave height and T_p the dominant wave period of the sea state. Offshore decisions are then based on weather forecasts expressed in terms of H_s, T_p and wave direction. The forecasted sea state

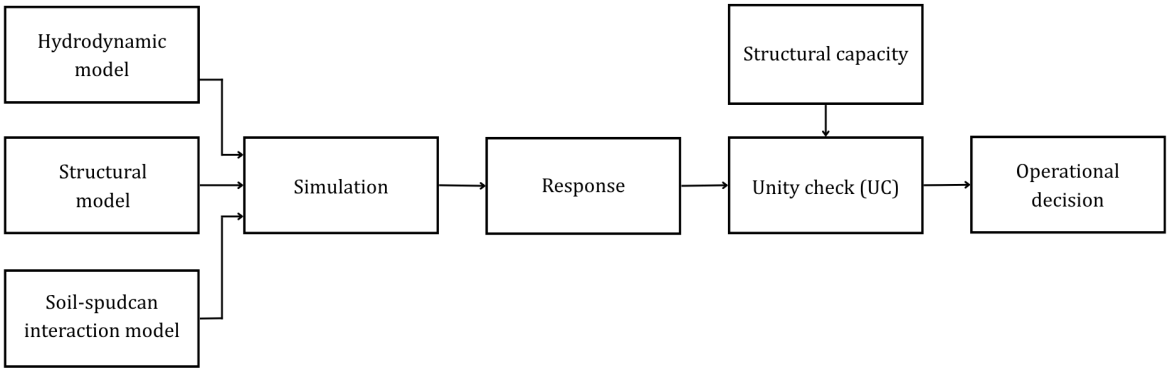

Figure 2.5: Current workability process based on (Holland & Hoogeveen, 2023)

is then compared with the allowable limits to determine whether the installation activity can proceed (Ringsberg et al., 2017).

Because of the stochastic nature of irregular wave loading, multiple time-domain simulations are commonly required for the same environmental condition. The resulting responses may then be evaluated statistically to define conservative but representative workability limits. Although this approach is physically detailed, it makes GoL assessment computationally demanding, especially when many combinations of H_s, T_p wave direction, water depth and soil condition must be assessed.

2.4 Energy-based perspective for GoL workability assessment

Existing methods have progressed from simple limits to detailed site-specific simulations that derive impact loads, unity checks and allowable sea states, but mainly after detailed analysis has been performed. Due to the complexity of the problem, there is value in considering alternative perspectives. Previous studies have demonstrated the potential of an energy-based approach to explain the relationship between vessel motion, energy transfer and impact loads.

2.4.1 Existing simplified energy-based approaches

The DNV simplified bottom impact method, introduced in section 2.3.1, is actually based on an energy approach. It estimates the impact force by assuming that the rotational energy of the jack-up is absorbed by the leg and supporting hull structure during touchdown. This links the resulting force to the vessel motion and the stiffness of the leg-support system. As already mentioned, the method is based on many conservative assumptions and thus gives limited insight into the detailed time-dependent energy transfer during touchdown.

Vazquez et al. (2016) build on this DNV approach by relating the vessel motion before touchdown to the resulting peak impact force. Their approach focuses on the downward spudcan velocity (DSV), which combines the vertical contribution from heave with the rotational contribution from roll or pitch. Since the kinetic energy available at impact is related to velocity, DSV provides a physically meaningful indicator for touchdown severity.

The study shows that peak impact loads generally increase with increasing DSV, indicating that the pre-impact motion state of the spudcan contains relevant information about the expected impact response. This supports the use of energy-related quantities as indicators for GoL

assessment. However, the approach remains focused on a simplified relation between pre-impact velocity and peak impact load, rather than on the complete time-dependent energy transfer during touchdown.

2.4.2 Opportunities for an energy interpretation

Vazquez et al. (2016) present valuable results by using energy principles to explain the origin of impact loads. However, their approach does not analyse energy transfer during the complete GoL sequence as a time-dependent response quantity, nor does it investigate how energy is transferred, stored and dissipated between vessel motion, leg deformation, contact work and soil-spudcan interaction during touchdown.

This limitation provides an opportunity to extend existing GoL assessment methods by treating energy as a response quantity within detailed GoL simulations. Modern GoL simulations already provide the required outputs, including vessel motions, hydrodynamic loads, soil reactions and structural response. These outputs can be used to evaluate how the system's mechanical energy changes during the operation and to investigate energy-based quantities in both the free-floating and impact phases.

In the impact phase, energy can be evaluated as a time-dependent quantity during touchdown. This makes it possible to investigate whether energy transfer during touchdown provides an indicator for transient impact severity. Seabed contact can be disabled to evaluate the no-impact energy response before touchdown occurs. This response can be analysed for the same wave seeds used in the impact-enabled simulations, and for longer free-floating simulations used to characterise steady-state energy behaviour across environmental cases.

The proposed energy-based model is intended to complement the current industrial assessment workflow. While unity checks remain essential for operational decision-making, energy-based quantities may provide additional insight into touchdown severity and may indicate whether the response contains information about allowable GoL conditions before impact occurs.

2.5 Concluding remarks

This chapter reviewed the physical background, existing assessment methods and energy-based interpretation of jack-up GoL workability. The main conclusions are:

- **Physical problem:** GoL is a transient and coupled process in which the jack-up transitions from a free-floating condition to seabed support. During touchdown, wave-induced vessel motions, leg flexibility, seabed contact and nonlinear soil-spudcan interaction determine how impact loads develop.
- **Existing methods:** GoL assessment methods have developed from simplified environmental and motion limits toward detailed site-specific simulations. Current industrial practice combines hydrodynamic, structural and soil-spudcan models to calculate impact loads, unity checks and allowable sea states for operational decision-making.
- **Limitation:** Although current simulation-based methods provide detailed and reliable workability limits, they can become computationally demanding when many environmental cases and irregular-wave realisations must be assessed. In addition, conventional outputs such as peak loads and unity checks give limited insight into the underlying energy transfer during touchdown.

- **Gap and motivation:** Existing energy-based approaches show that touchdown impact is physically related to mechanical energy, but they generally rely on simplified assumptions or limited energy-related quantities. This motivates the present thesis, which evaluates global mechanical energy as a time-dependent response quantity within detailed GoL simulations, aiming to link pre-impact vessel motion, energy transfer during touchdown and resulting impact severity.

Modelling framework 3

The assessment of impact loads during the GoL is based on a description of the vessel motions and responses induced by environmental conditions. These motions are translated into the energy contained within the system. The evolution of this energy throughout the GoL process, and in particular during the impact phase, serves as a measure for the severity of the impact. This chapter presents the structure of the modelling framework and the formulation used to compute and evaluate the associated energy response.

3.1 Energy-based simulation workflow

The modelling framework adopted in this thesis is based on the framework developed by Holland and Hoogeveen (2023), and combines hydrodynamic input from OrcaWave (Orcina Ltd, 2025b) with time-domain simulations in OrcaFlex (Orcina Ltd, 2025a) to obtain the vessel motions and hydrodynamic forces under specified environmental conditions. These results are subsequently used in the energy formulation to evaluate the total energy and power balance during the GoL operation (Figure 3.1). The energy equation defines the total mechanical energy of the vessel as the sum of kinetic and potential energy, thereby providing a global scalar description of the vessel response. The power balance relates the time rate of change of this energy to the difference between incoming and dissipated power.

As introduced in section 1.1, the free-floating and impact phases are distinguished. In the remainder of this thesis, a distinction is made between physical GoL phases and numerical simulation types. The terms free-floating phase, impact phase and lifting phase refer to stages of the GoL operation. The terms free-floating simulation and impact simulation refer to specific numerical simulations used in the energy analysis.

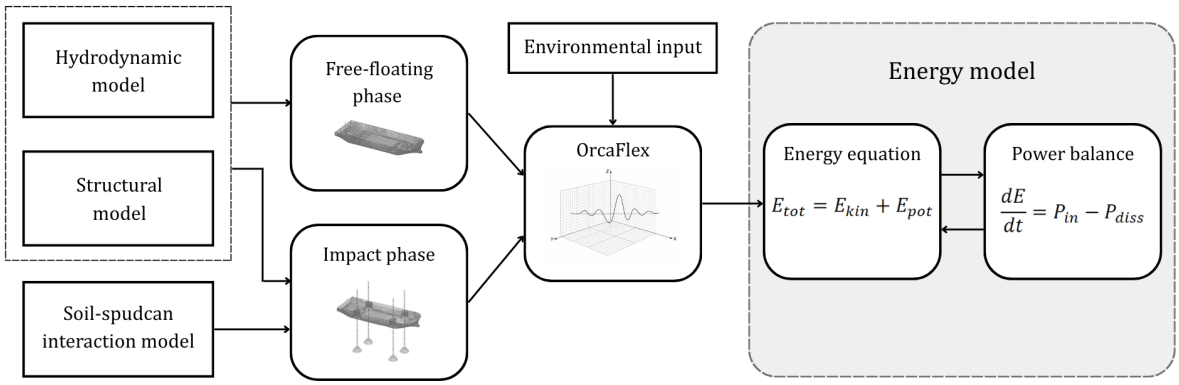

Figure 3.1: Schematic overview of simulation workflow

3.2 Model inputs and coordinate transformations

This section introduces the modelling components required to construct the time-domain GoL simulations. The hydrodynamic, environmental and coordinate-system inputs provide the means to translate irregular wave conditions into vessel motions, loads and energy quantities. These inputs therefore form the practical basis of the simulation framework developed in the following sections.

3.2.1 Hydrodynamic input

The model uses hydrodynamic input obtained from an OrcaWave diffraction–radiation analysis. The analysis is based on linear potential flow theory and a boundary element method (BEM), following Journée and Massie (2008).

The following hydrodynamic quantities are used as model input. The matrix quantities are formulated in the six rigid-body degrees of freedom of the vessel and are therefore (6×6) symmetric matrices:

- $\mathbf{M}$ – **mass matrix:** structural mass and inertia matrix based on the vessel mass, centre of gravity and moments of inertia.
- $\mathbf{K}$ – **hydrostatic stiffness matrix:** restoring stiffness matrix based on the hydrostatic pressure distribution over the wetted hull.
- $\mathbf{A}(\omega)$ – **added mass matrix:** frequency-dependent added-mass coefficients obtained from the radiation analysis.
- $\mathbf{C}(\omega)$ – **radiation damping matrix:** frequency-dependent radiation-damping coefficients obtained from the radiation analysis.
- $\mathbf{F}_{\mathrm{exc}}(\omega)$ – **wave-excitation loads:** first-order wave-excitation forces and moments obtained from the diffraction analysis.
- $\mathrm{RAO}_{\mathrm{load}}(\omega)$ – **load response-amplitude operator**: complex load RAO obtained from the diffraction analysis. It relates the complex wave amplitude to the complex excitation-force amplitude:

$$\mathrm{RAO}_{\mathrm{load}}(\omega) = \frac{\hat{\mathbf{F}}_{\mathrm{exc}}(\omega)}{\hat{\eta}}.$$

- $\mathrm{RAO}_{q_j}(\omega)$ – **motion response-amplitude operator**: complex motion RAO obtained from the diffraction–radiation analysis for degree of freedom j. It relates the complex wave amplitude to the complex motion-response amplitude:

$$\mathrm{RAO}_{q_j}(\omega) = \frac{\hat{q}_j(\omega)}{\hat{\eta}}.$$

3.2.2 Environmental input

The environmental input is defined by irregular wave conditions. Each environmental case is specified by the following sea-state parameters:

- H_s – **significant wave height:** characteristic wave height of the irregular sea state.
- T_p – **peak period:** wave period corresponding to the peak of the wave spectrum.

- β − **wave direction:** direction of wave propagation relative to the vessel heading.

The irregular wave field is represented using a JONSWAP spectrum. This spectrum is used to represent combined sea-state conditions associated with swell and wind-wave components. The spectral shape is governed by H_s, T_p and the peakedness factor γ. In this study, a constant value of $\gamma = 3.3$ is used for all simulations, corresponding to a standard JONSWAP formulation (Journée & Massie, 2008).

For a fixed combination of H_s, T_p, γ and wave direction β, different random seeds are used to generate different phase realisations of the same sea state. The seed changes the time-domain wave elevation and wave-force history, while the underlying sea-state parameters remain unchanged.

To avoid transient start-up effects at the beginning of the simulations, the wave-induced loading is gradually introduced using a ramping function, resulting in a smooth increase in wave elevation and associated hydrodynamic loads.

Only wave-induced loading is considered in the present model. Wind loads and current loads are excluded from the environmental input.

3.2.3 Reference frames and transformations

In the time-domain simulations performed in OrcaFlex, different reference frames are employed for the representation of kinematic quantities and forces. The vessel motions, denoted by $\mathbf{u}(t)$, are defined with respect to the inertial (fixed) global coordinate system G. In contrast, the hydrodynamic and structural loads reported by the simulation are expressed in a local body-fixed coordinate system L, typically located at the aft keel on the vessel centerline.

To ensure consistency, the forces computed in the local frame L must be transformed to the centre of gravity (COG) and subsequently expressed in the global frame G. This transformation is performed using:

$$\mathbf{F}_G = \mathbf{T}\,\mathbf{F}_L$$

where $\mathbf{T}$ is the adjoint transformation matrix, as described by Lynch and Park (2017):

$$\mathbf{T} = \begin{bmatrix} \mathbf{R} & \mathbf{0} \\ -\mathbf{R}[\mathbf{r}]_\times & \mathbf{R} \end{bmatrix}$$

This transformation matrix accounts for both rotational and translational effects, enabling the mapping of forces and moments from the local reference point to the COG and from the body-fixed frame to the global frame.

The rotation matrix $\mathbf{R}$ transforms vectors from the local body-fixed coordinate system to the global coordinate system and describes the vessel orientation through roll, pitch, and yaw (Fossen, 2021).

The skew-symmetric matrix $[\mathbf{r}]_\times$ is defined as:

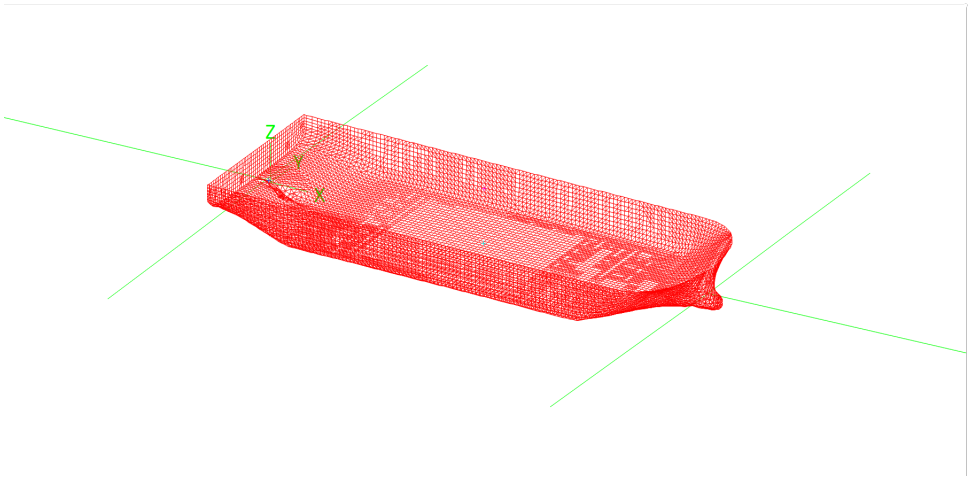

Figure 3.2: OrcaFlex model used for the free floating simulation: The legs are fully elevated and implicitly included in the simulation model.

$$[\mathbf{r}]_\times = \begin{bmatrix} 0 & -z & y \\ z & 0 & -x \\ -y & x & 0 \end{bmatrix}$$

where $\mathbf{r} = [x \ y \ z]^T$ represents the position vector from the local reference point L to the CoG. This matrix enables the representation of the moment contribution arising from a force applied at an offset location, through the cross-product operation (Fossen, 2021). The complete derivation of the adjoint transformation matrix $\mathbf{T}$ from the rotation $\mathbf{R}$ and the skew-symmetric matrix $[\mathbf{r}]_\times$ can be found in appendix A.

3.3 Time-domain model for energy analysis

In the time domain, the jack-up motion response is evaluated. The corresponding external force and moment components are first formulated according to the OrcaFlex conventions. Based on this force representation, the governing energy equation is derived by relating the instantaneous generalized forces to the translational and rotational velocities of the vessel.

3.3.1 Equation of motion and force decomposition

The geometry of the hull is defined by a surface mesh that describes the wetted shape of the vessel. This mesh provides the spatial representation of the hull and defines how external loads are distributed over the structure. During the simulation, the resulting forces and moments are applied at the vessel reference point L, governing the translational and rotational motion of the rigid body. These loads are subsequently transformed according to the adjoint transformation described in section 3.2.3.

The jack-up motion is described in generalized coordinates $\mathbf{u} = [x, y, z, \phi, \theta, \psi]^T$, where x, y, z denote translations and ϕ, θ, ψ denote roll, pitch and yaw. The corresponding generalized velocity and acceleration are denoted by $\mathbf{v} = \dot{\mathbf{u}}$ and $\mathbf{a} = \ddot{\mathbf{u}}$.

$$\mathbf{Ma} = \mathbf{F}_{\text{stiffness}} + \mathbf{F}_{\text{links}} + \mathbf{F}_{\text{rad}} + \mathbf{F}_{\text{other-damping}} + \mathbf{F}_{\text{wave}} \tag{3.1}$$

Conservative forces

- $\mathbf{F}_{\text{stiffness}}$ represents the hydrostatic restoring force, defined as a linear stiffness contribution acting on the vessel displacement:

  $$\mathbf{F}_{\text{stiffness}} = -\mathbf{Ku}$$

  where $\mathbf{K}$ is the hydrostatic stiffness matrix and $\mathbf{u}$ the displacement vector from the equilibrium position. This term represents the restoring force due to buoyancy and contributes to the potential energy of the system, and is therefore treated as a conserved energy term.

- $\mathbf{F}_{\text{links}}$ represents the restoring forces arising from the connection system, modelled using a simplified spring-based representation of the Dynamic Positioning (DP) system (section 2.1.1).

  The restoring behaviour is described by a global mooring stiffness matrix, denoted as $\mathbf{K}_{\text{mooring}}$, obtained by combining the individual link stiffness contributions and reducing the system using Guyan reduction (Guyan, 1965). This results in an equivalent stiffness matrix defined at the vessel level, which contributes to the potential energy and is therefore treated as a conserved energy term.

Dissipative forces

- $\mathbf{F}_{\text{rad}}$ is the radiation force, expressed as a combined frequency-dependent contribution of added mass and radiation damping: $-\mathbf{A}(\omega)\boldsymbol{a} - \mathbf{C}(\omega)\mathbf{v}$.

  For use in the time-domain model, this frequency-dependent formulation is replaced by equivalent constant coefficients $\mathbf{A}_{eq}$ and $\mathbf{C}_{eq}$. These are obtained using the power-based averaging method proposed by (Fossen, 2025). The equivalent coefficients are obtained by weighting the frequency-dependent coefficients with a normalized wave spectrum:

  $$\mathbf{A}_{eq} = \int_0^{\omega_{max}} \mathbf{A}(\omega) S_{\zeta,N}(\omega)\, d\omega$$
  $$\mathbf{C}_{eq} = \int_0^{\omega_{max}} \mathbf{C}(\omega) S_{\zeta,N}(\omega)\, d\omega$$

  A separate frequency independent representation of $\mathbf{A}$ and $\mathbf{C}$ is required to preserve the physical distinction between energy storage (added mass) and energy dissipation (radiation damping), which is essential for a consistent energy-based assessment of the system response.

- $\mathbf{F}_{\text{other-damping}}$ represents additional damping effects not captured by the linear radiation model. In the present simulations, this contribution is only included in the roll degree of freedom, where these effects are most pronounced. The damping is taken as 5% of the critical damping, which corresponds to the minimum damping required to prevent oscillatory motion. This coefficient is denoted by L and represents the linear damping coefficient, such that the other damping force is expressed as $-\mathbf{Lv}$.

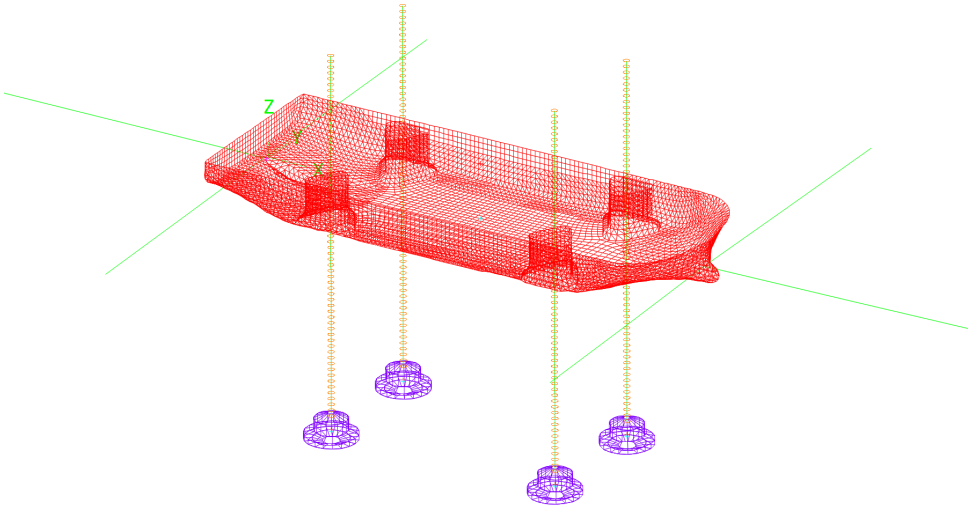

Figure 3.3: OrcaFlex model used for the impact simulation: The legs are fully extracted and explicitly included in the simulation model

External forces

- $\mathbf{F}_{\text{wave}}$ are the forces and moments on the vessel due to the first order wave load that represent the excitation force $\mathbf{F}_{\text{exc}}$.

3.3.2 System matrices for free-floating and impact configurations

In the impact simulation, the jack-up is modelled as a coupled system consisting of the hull, legs, and spudcans, as illustrated in Figure 3.3. In contrast to the free-floating model, the legs and their interaction with the seabed are explicitly included, allowing the transfer of loads from the hull to the soil to be captured.

For the impact energy formulation, the system properties $\mathbf{M}$, $\mathbf{A}$ and $\mathbf{K}$ must represent the jack-up in its lowered-leg configuration. This differs from the free-floating configuration, where the legs are fully elevated and are implicitly included in the properties of the vessel.

Mass matrix For each configuration, the mass matrix is defined with respect to the COG of that configuration and expressed in the local vessel coordinate system L. The generalized structural mass matrix can therefore be written as

$$\mathbf{M} = \begin{bmatrix} m\mathbf{I}_3 & \mathbf{0} \\ \mathbf{0} & \mathbf{I}_G \end{bmatrix}$$

where m is the total mass of the considered configuration, $\mathbf{I}_3$ is the 3×3 identity matrix, and $\mathbf{I}_G$ is the inertia tensor about the corresponding COG.

The free-floating OrcaFlex model provides the combined mass properties of the hull and the elevated legs. To obtain the hull-only mass properties, the contribution of the elevated legs is removed from this combined system. The legs are then reintroduced explicitly in their lowered configuration. Since the hull and lowered-leg mass properties must be expressed about a common reference point before they can be combined, the required transformations are performed using

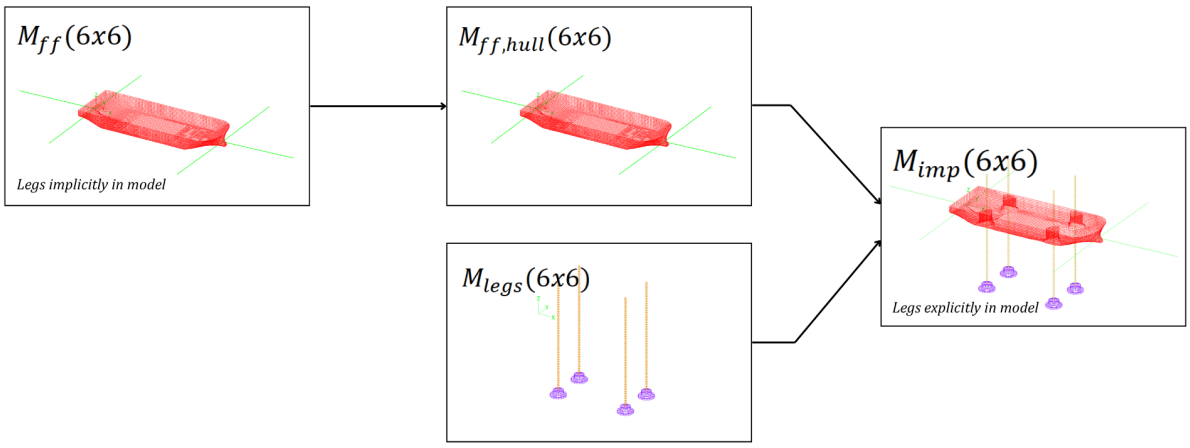

Figure 3.4: Construction of the mass matrix corresponding to the impact model.

the parallel axis theorem. The impact model mass properties are subsequently obtained by combining the hull contribution with the transformed mass properties of the lowered legs, as illustrated in Figure 3.4 (Hibbeler, 2016a). The full derivation of the mass matrix is provided in Appendix B.

Hydrostatic stiffness matrix The stiffness matrix is formulated in a reduced form by retaining heave, roll, and pitch, together with the coupling between heave and pitch. The matrix therefore takes the form

$$\mathbf{K} = \begin{bmatrix} K_{zz} & 0 & K_{z\theta} \\ 0 & K_{\phi\phi} & 0 \\ K_{z\theta} & 0 & K_{\theta\theta} \end{bmatrix}$$

The diagonal terms represent the uncoupled hydrostatic stiffness contributions while the off-diagonal term $K_{z\theta}$ captures the coupling between vertical motion and pitch.

The heave stiffness K_{zz} is obtained directly from the free-floating model. It is primarily governed by hydrostatic restoring forces associated with the waterplane area which remains the same in the impact-model.

The pitch and roll stiffness terms, $K_{\theta\theta}$ and $K_{\phi\phi}$, are determined from the natural periods obtained through modal analysis in OrcaFlex. For each rotational degree of freedom, the stiffness is related to the corresponding natural period and mass moment of inertia according to

$$T_n^{(i)} = 2\pi\sqrt{\frac{M_i}{K_i}}, \quad i \in \{\theta, \phi\},$$

which allows the stiffness terms to be computed directly from the identified modal properties.

The heave–pitch coupling term $K_{z\theta}$ is included to account for the geometric offset between the centre of buoyancy and the centre of gravity. A vertical displacement produces a restoring buoyancy force acting through the centre of buoyancy. If this force does not pass through the centre of gravity, it generates a restoring pitch moment. The magnitude of this coupling term is therefore governed by the horizontal distance between these reference points.

Added mass and radiation damping matrix The hydrodynamic equivalent added-mass matrix $\mathbf{A}_{\text{eq}}$ and equivalent damping matrix $\mathbf{C}_{\text{eq}}$ are obtained using the same power-based averaging method described in section 3.3.1. However, the underlying frequency-dependent hydrodynamic coefficients $\mathbf{A}(\omega)$ and $\mathbf{C}(\omega)$ are taken from the impact model configuration.

3.3.3 Representation of leg and soil–spudcan interaction

The legs are rigidly attached to the hull body and discretised into nodes connected by segments. These nodes represent discrete points along the structure at which mass and hydrodynamic loads are lumped, and where forces and moments are applied, while the segments capture the structural behaviour between them (Orcina Ltd, 2025a). The spudcans are modelled as 6D buoys attached to the lower end of each leg, representing rigid bodies with six degrees of freedom, allowing independent translation and rotation in all directions.

The leg and buoy properties include mass and inertia, while environmental loads, such as hydrodynamic forces, act along the legs and at the spudcans. Upon contact with the seabed, the spudcans experience both vertical and horizontal impact forces at the contact interface. These forces are transmitted through the legs to the hull at the leg–hull connection, where they contribute to the global force and moment balance. Consequently, the resultant impact force acting through the spudcans is included in the external force vector in equation 3.1 as the impact force term, $\mathbf{F}_{\text{imp}}$.

3.3.4 Strain energy in legs during touchdown

For the impact model, the forces and moments transmitted from the legs and spudcans to the hull require an additional interpretation. The translational force components acting at the leg–hull interface are treated as external force contributions to the hull force balance. The moment contribution, however, induces bending of the leg and therefore introduces elastic energy storage in the structure. This stored elastic energy is referred to as strain energy.

The bending strain energy in a beam is given by (Hibbeler, 2016b)

$$E_{\text{strain}} = \int_0^L \frac{M(x)^2}{2EI}\, dx, \tag{3.2}$$

where $M(x)$ is the bending moment distribution along the leg, E is the Young's modulus, I is the second moment of area, and L is the leg length.

In OrcaFlex, the legs are modelled as axially and torsionally rigid elements, such that only bending deformations contribute to the elastic energy. Furthermore, bending stiffness is considered in both the x- and y-directions. Assuming the leg can be idealised as a clamped-free beam subjected to an equivalent transverse load at the spudcan, the bending moment varies linearly along the leg. In terms of the bending moments at the leg–hull interface, this yields

$$E_{\text{strain},x} = \frac{M_{LH,x}^2 L}{6EI_x}, \qquad E_{\text{strain},y} = \frac{M_{LH,y}^2 L}{6EI_y}. \tag{3.3}$$

The full derivation of equations 3.2 and 3.3 can be found in Appendix C. The total strain energy stored in the leg is then obtained by summing the contributions from both bending directions. This strain energy represents the portion of the impact energy that is temporarily stored as bending deformation of the legs and is therefore included as an additional mechanical energy term in the formulation.

3.4 Governing energy equations for GoL analysis

The preceding sections define the system properties, force contributions and strain-energy terms required to describe the energy response of the jack-up during the GoL operation. This section combines these components into the final energy formulations used in the analysis, distinguishing between the free-floating configuration and the impact configuration. The resulting equations provide the basis for evaluating the global mechanical energy of the vessel and, during touchdown, the additional strain energy stored in the legs.

3.4.1 Free-floating and impact energy formulations

The input properties presented in section 3.3.1 consist of terms with different energetic roles. The mass $\mathbf{M}$, equivalent added-mass $\mathbf{A_{eq}}$ and stiffness $\mathbf{K}$ terms represent energy stored in the vessel-fluid system, while the excitation $\mathbf{F_{exc}}$ and damping terms $\mathbf{C_{eq}}$ (and $\mathbf{L}$) represent energy transfer. The inertia terms define the kinetic energy, whereas the stiffness term defines the potential energy associated with displacement from equilibrium. For an undamped vibrating system, kinetic and potential energy are exchanged without loss of total mechanical energy (Chopra, 2020; S. S. Rao, 2017).

The final energy formulations used in the analysis are summarized below. The subscripts ff and imp denote quantities associated with the free-floating and impact configurations, respectively.

Free-floating energy formulation For the free-floating configuration, the system is defined by

$$(\mathbf{M}_{\text{ff}} + \mathbf{A}_{\text{eq,ff}})\mathbf{a} + (\mathbf{K}_{\text{ff}} + \mathbf{K}_{\text{mooring}})\mathbf{u} = \mathbf{F}_{\text{wave}} - \mathbf{C}_{\text{eq,ff}}\mathbf{v} - \mathbf{L}\mathbf{v}.$$

Premultiplying by $\mathbf{v}^T$ results in the corresponding mechanical energy:

$$E_{\text{ff}} = \frac{1}{2}\mathbf{v}^T \left(\mathbf{M}_{\text{ff}} + \mathbf{A}_{\text{eq,ff}}\right)\mathbf{v} + \frac{1}{2}\mathbf{u}^T \left(\mathbf{K}_{\text{ff}} + \mathbf{K}_{\text{mooring}}\right)\mathbf{u}. \tag{3.4}$$

The power balance is

$$\frac{dE_{\text{ff}}}{dt} = \mathbf{v}^T\mathbf{F}_{\text{wave}} - \mathbf{v}^T\mathbf{C}_{\text{eq,ff}}\boldsymbol{v} - \mathbf{v}^T\mathbf{L}\mathbf{v}. \tag{3.5}$$

Impact energy formulation For the impact phase, the lowered-leg configuration is used:

$$(\mathbf{M}_{\text{imp}} + \mathbf{A}_{\text{eq,imp}})\mathbf{a} + (\mathbf{K}_{\text{imp}} + \mathbf{K}_{\text{mooring}})\mathbf{u} = \mathbf{F}_{\text{hyd}} + \mathbf{F}_{\text{imp}}$$

The mechanical energy is

$$E_{\text{global,imp}} = \frac{1}{2}\mathbf{v}^T \left(\mathbf{M}_{\text{imp}} + \mathbf{A}_{\text{eq,imp}}\right)\mathbf{v} + \frac{1}{2}\mathbf{u}^T \left(\mathbf{K}_{\text{imp}} + \mathbf{K}_{\text{mooring}}\right)\mathbf{u}. \tag{3.6}$$

The total impact energy used in the analysis is then

$$E_{\text{imp}} = E_{\text{global,imp}} + E_{\text{strain}}.$$

In principle, the rate of change of the impact mechanical energy can be interpreted as the sum of a hydrodynamic power contribution and an impact power contribution:

$$\frac{\mathrm{d}E_{\text{global,imp}}}{\mathrm{d}t} = P_{\text{hyd}} + \mathbf{v}^T\mathbf{F}_{\text{imp}}.$$

The term $\mathbf{v}^T\mathbf{F}_{\text{imp}}$ represents the power exchanged through soil–spudcan interaction. It accounts for the work rate associated with impact forces, soil deformation and load transfer into the legs during touchdown.

In the present implementation, this impact power balance is used only as a conceptual interpretation, because constructing a fully consistent generalized impact-force vector for the complete coupled hull–leg–soil system is outside the scope of the present model. Instead, the impact simulation analysis evaluates the mechanical energy obtained from the impact model mass, added-mass and stiffness matrices, together with the simulated kinematics.

3.4.2 Harmonic-response method for energy-balance verification

To verify the implemented equation of motion and corresponding energy formulation, a frequency-domain harmonic-response case is formulated.

For a harmonic response at the same frequency, the frequency-domain equation of motion is written as (Journée & Massie, 2008):

$$\left[-\omega^2\left(\mathbf{M} + \mathbf{A}(\omega)\right) + i\omega\mathbf{C}(\omega) + \mathbf{K}\right]\hat{\mathbf{u}}(\omega) = \hat{\mathbf{F}}_{\text{exc}}(\omega) \tag{3.7}$$

where the bracketed term represents the complex impedance matrix $\hat{\mathbf{Z}}(\omega)$ and $\hat{\mathbf{u}}$ is the complex displacement-response amplitude vector. The sign convention in this expression follows the adopted $e^{i\omega t}$ harmonic convention. For the verification case, the frequency-dependent hydrodynamic coefficients are evaluated at the imposed harmonic frequency, so that the reconstructed response can be compared directly with the implemented time-domain energy balance.

Equation 3.7 is solved for $\hat{\mathbf{u}}$ and then used to reconstruct the time-domain displacement, velocity and acceleration:

$$\begin{aligned}
\mathbf{u}(t) &= \Re\left\{\hat{\boldsymbol{u}}e^{i(\omega t)}\right\},\\
\mathbf{v}(t) &= \Re\left\{i\omega\hat{\boldsymbol{u}}e^{i(\omega t)}\right\},\\
\mathbf{a}(t) &= \Re\left\{-\omega^2\hat{\boldsymbol{u}}e^{i(\omega t)}\right\}.
\end{aligned}$$

Similarly, the time-dependent excitation-force vector is reconstructed as

$$\mathbf{F}_{\text{exc}}(t) = \Re\left\{\hat{\mathbf{F}}_{\text{exc}}(\omega)e^{i(\omega t)}\right\}.$$

These reconstructed displacement, velocity, acceleration and excitation-force signals are substituted into the implemented energy and power equations. The resulting energy balance is evaluated in section 4.1.

Energy-based analysis 4

This chapter presents the results of the developed energy-based model. First, the energy formulation is verified in the frequency domain using RAO-based responses. Subsequently, time-domain simulations are analysed for three representative sea states, demonstrating the energy balance and system behaviour under different wave conditions, for both the free-floating and the impact simulation.

4.1 Frequency-domain verification results

This section presents the verification of the energy formulation introduced in Section 3.4.2 using frequency-domain response data. The objective is to demonstrate that the implemented energy equation is consistent with the underlying hydrodynamic model.

4.1.1 Harmonic reconstruction of response

A regular incoming wave is represented using complex notation as

$$\eta(t) = \Re\left\{\hat{\eta}e^{i\omega t}\right\}, \qquad \hat{\eta} = \zeta_a e^{i\epsilon},$$

where ζ_a is the wave amplitude, ω is the wave angular frequency, and ϵ is the wave phase angle.

For a selected wave period $T = 12\,\mathrm{s}$, the vessel response is reconstructed from the frequency-domain formulation presented in section 3.4.2. A unit wave amplitude of $\zeta_a = 1\,\mathrm{m}$ is applied, and the corresponding angular frequency is defined as

$$\omega = \frac{2\pi}{T}.$$

For the present analysis, the vessel is subjected to harmonic wave excitation propagating in the longitudinal direction. Owing to the geometric symmetry of the vessel with respect to its longitudinal centreplane, and the selected wave heading, the response is symmetric about this plane. Consequently, the dominant responding degrees of freedom are surge (x), heave (z), and pitch (θ).

The reconstructed response exhibits purely harmonic behaviour, as expected for a linear system subjected to single-frequency regular wave excitation. The plotted signals are normalized for

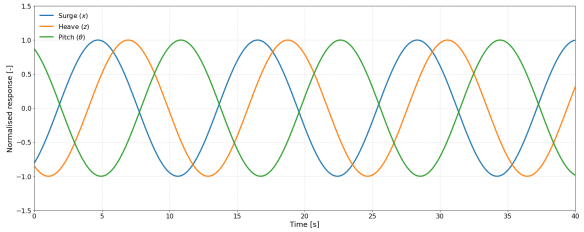

Figure 4.1: Reconstructed vessel response at $T = 12\,\mathrm{s}$

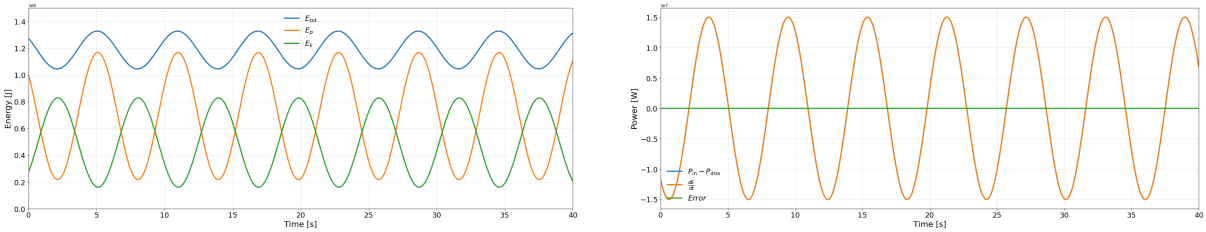

(a) Total energy over time

(b) Power balance verification

Figure 4.2: Energy and power balance for harmonic excitation ($T = 12\,\mathrm{s}$)

visualization and therefore illustrate the relative phase differences rather than the physical response amplitudes. These phase differences originate from the complex motion RAOs used in the response reconstruction.

4.1.2 Energy balance verification

Using the reconstructed time signals in section 3.4.2, the mechanical energy of the system and the associated power terms are evaluated according to the energy formulation. The excitation-force time series is reconstructed according to the harmonic-response method introduced in equation 3.7, using the complex load and motion RAOs obtained from OrcaWave as hydrodynamic input.

The results show that the kinetic and potential energy oscillate periodically and are out of phase, reflecting the continuous exchange of energy between inertia and restoring forces that is characteristic of vibrating systems (K. R. Rao, 2016). The total mechanical energy varies over time due to the combined effect of wave-induced energy input and dissipation, where damping removes part of the energy from the system during each cycle (Figure 4.2a). To verify the consistency of the energy formulation, the rate of change of total mechanical energy is compared with the net power input to the system (Figure 4.2b).

This demonstrates that the energy-based formulation is fully consistent with the governing equation of motion and provides a reliable basis for the subsequent time-domain analyses.

4.2 Time-domain energy response results

This section presents the results of the time-domain simulations described in section 3.3. Three representative wave conditions are considered to investigate the influence of wave direction and spectral composition on the system response and energy behaviour.

The following wave conditions are analysed:

- **Case 1 - Head sea:** ($H_s = 2\mathrm{m}$, $T_p = 12\mathrm{s}$, $0°$)
- **Case 2 - Oblique sea:** ($H_s = 2\mathrm{m}$, $T_p = 12\mathrm{s}$, $30°$)
- **Case 3 - Bi-modal sea:** ($H_s = 3\mathrm{m}$, $T_p = 12\mathrm{s}$, $30°$) — ($H_s = 1\mathrm{m}$, $T_p = 8\mathrm{s}$, $270°$)

Cases 1 and 2 represent unimodal swell-dominated sea states, in which the wave energy is concentrated around a single peak period and direction. Case 3 represents a bi-modal sea state, consisting of a long-period swell component and a shorter-period wind-sea component propagating from a different direction.

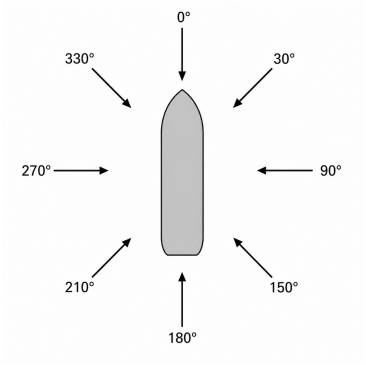

Figure 4.3: Wave direction convention

4.2.1 Energy response of the free-floating simulation

The time evolution of the mechanical energy for the three cases are shown in Figures 4.5 and 4.6. In all cases, the energy signal exhibits an irregular but clearly oscillatory behaviour. Despite the differences in wave conditions, the overall structure of the energy response remains similar across all cases. However, the small differences observed between the cases are consistent with the expected changes in the response under varying wave conditions.

Comparing Case 1 and Case 2 shows that introducing an oblique wave direction results in a smoother and more continuous energy response. While the head-sea condition primarily excites surge, heave, and pitch motions, the oblique sea state additionally activates sway, roll, and yaw. The increased coupling between degrees of freedom redistributes the wave-induced energy over multiple motion components, reducing the concentration of energy in distinct peaks and leading to a more persistent energy response over time.

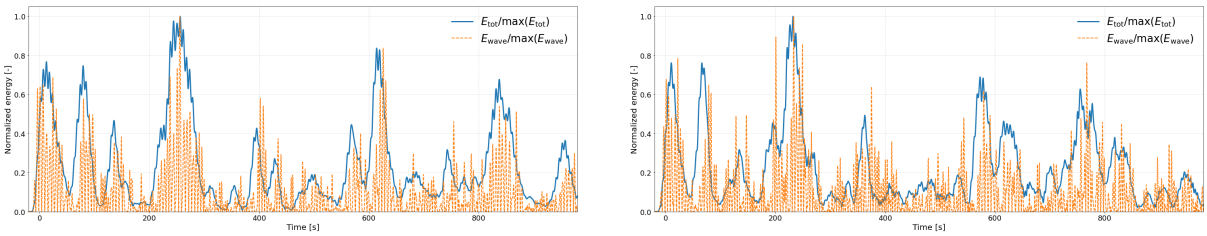

(a) Case 1

(b) Case 3

Figure 4.4: Normalized total mechanical energy and wave-elevation-squared indicator for Cases 1 and 3

To relate the global energy response to the incoming irregular wave signal, the normalized total mechanical energy response is compared with the normalized wave-elevation-squared indicator $\eta(t)^2$, as shown in Figure 4.4. In linear wave theory, the mean wave energy per unit horizontal sea-surface area is proportional to the variance of the free-surface elevation (Journée & Massie, 2008). Therefore, $\eta(t)^2$ is used here as a simple indicator of energetic wave groups.

For the unimodal condition in Case 1, peaks in E_{tot} tend to occur during periods with elevated $\eta(t)^2$. For the bimodal condition in Case 3, this relation becomes less direct: short peaks in the wave-energy indicator do not always lead to large energy responses, while E_{tot} also contains broader elevated intervals. This shows that energetic wave groups do not necessarily correspond directly to the most energetic vessel-response intervals.

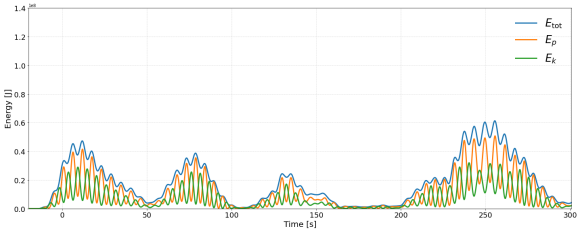

(a) Energy balance for Case 1.

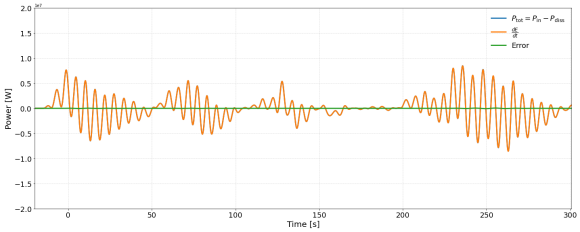

(b) Power balance for Case 1.

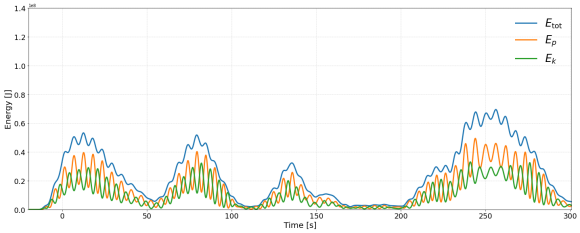

(c) Energy balance for Case 2.

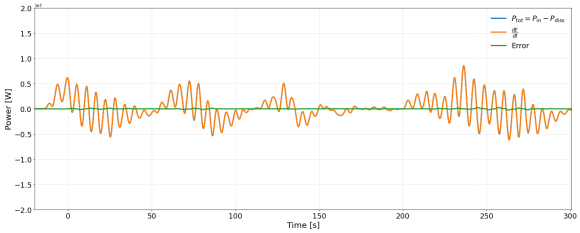

(d) Power balance for Case 2.

Figure 4.5: Energy and power balance for Case 1 and Case 2.

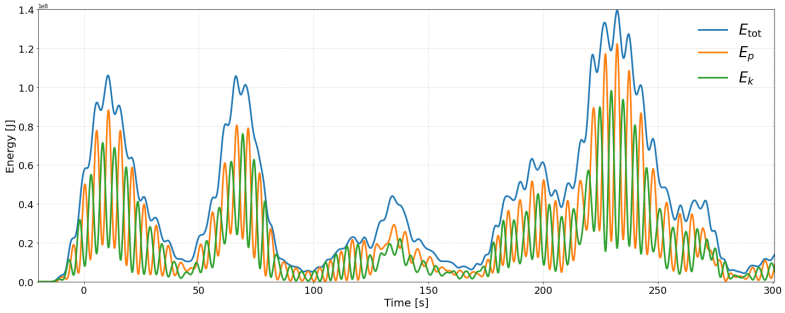

(a) Energy balance for Case 3.

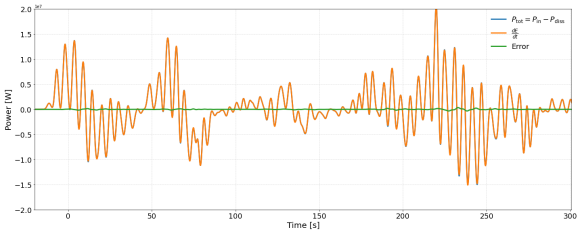

(b) Power balance for Case 3.

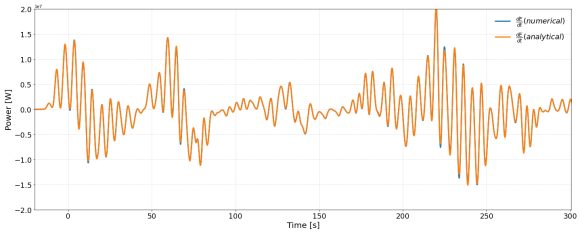

(c) Numerical analysis for Case 3.

Figure 4.6: Energy and power balance for Case 3.

While $\eta(t)^2$ is used to identify energetic wave groups within a single realization, the relative total wave-energy level between cases can be estimated from the significant wave height. For Case 1, the energy level is proportional to 2^2, whereas for Case 3 the two independent wave components give a combined contribution proportional to $3^2 + 1^2$. This results in

$$\frac{E_3}{E_1} = \frac{H_{s,3a}^2 + H_{s,3b}^2}{H_{s,1}^2} = \frac{3^2 + 1^2}{2^2} = 2.5.$$

Case 3 therefore contains approximately 2.5 times more linear wave energy per unit sea-surface area than Case 1. This higher total environmental energy level, combined with the broader spectral distribution, is consistent with the response plots, where larger peak values and more sustained energy levels are observed.

For all cases, the agreement between the rate of change of the free-floating mechanical energy and the corresponding power balance is very good, confirming the consistency of the energy formulation. Here, $P_{\text{tot}} = P_{\text{in}} - P_{\text{diss}}$ (from the figures) denotes the right-hand side of the power balance:

$$P_{\text{tot}} = \mathbf{v}^T \mathbf{F}_{\text{wave}} - \mathbf{v}^T \mathbf{C}_{\text{eq,ff}} \mathbf{v} - \mathbf{v}^T \mathbf{L} \mathbf{v}. \tag{4.1}$$

The RMSE check compares this force-based power quantity with the analytically determined $\mathrm{d}E_{\text{ff}}/\mathrm{d}t$, thereby verifying that the stored-energy formulation and the power formulation are mutually consistent.

The relative RMSE values are:

- Case 1: approximately 0.053%
- Case 2: approximately 0.483%
- Case 3: approximately 0.729%

The error remains small in all cases, demonstrating that the implemented energy formulation provides a robust and accurate description of the system behaviour under both unimodal and bi-modal wave conditions.

4.2.2 Energy response of the impact simulation

The energy balance in the impact simulation is extended with an additional energy contribution associated with the elastic deformation of the legs. This contribution is represented by the total strain energy E_{strain} which is obtained from the bending moments transmitted through the leg–hull connections.

Pre-impact Figure 4.7 shows the energy response of the impact simulation for the three cases. These cases show similar or slightly reduced total energy levels compared to the elevated-leg configurations. In addition, the energy response becomes smoother, with reduced fluctuations over time. The lower centre of gravity increases the metacentric height, resulting in greater hydrostatic stability and reduced rotational motion amplitudes. At the same time, the changed mass distribution modifies the moments of inertia and shifts the natural periods of the rigid-body modes. In particular, changes in the roll, pitch, and heave modes affect how strongly the vessel responds to the incoming wave excitation. Additional hydrodynamic damping associated with the lowered legs further contributes to a more gradual redistribution and dissipation of energy.

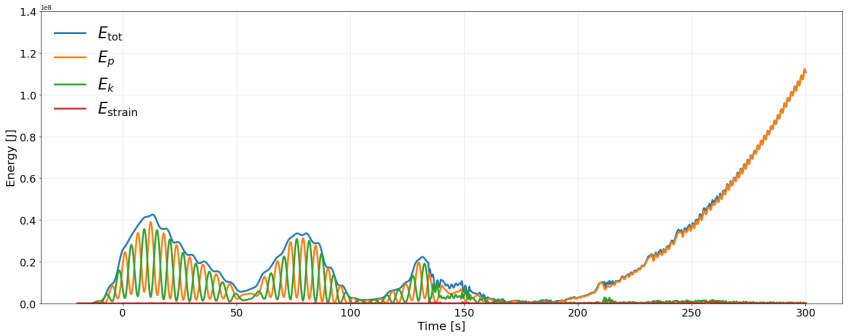

(a) Case 1

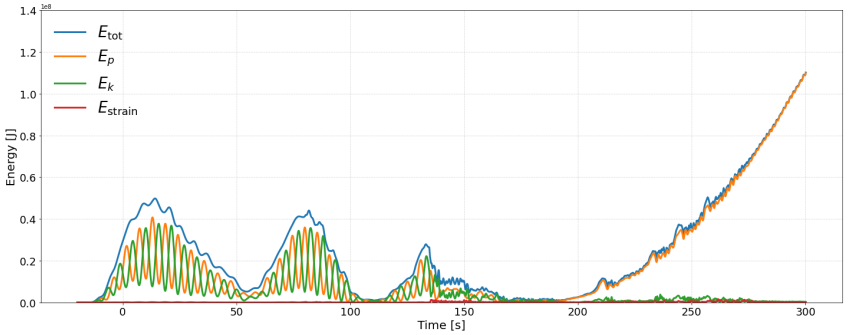

(b) Case 2

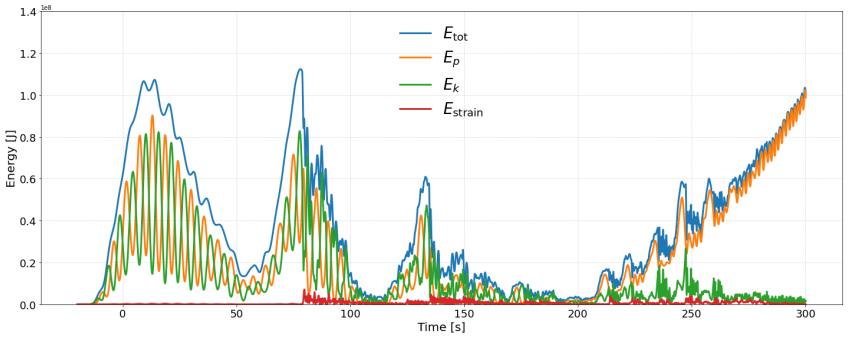

(c) Case 3

Figure 4.7: Energy response for Cases 1–3.

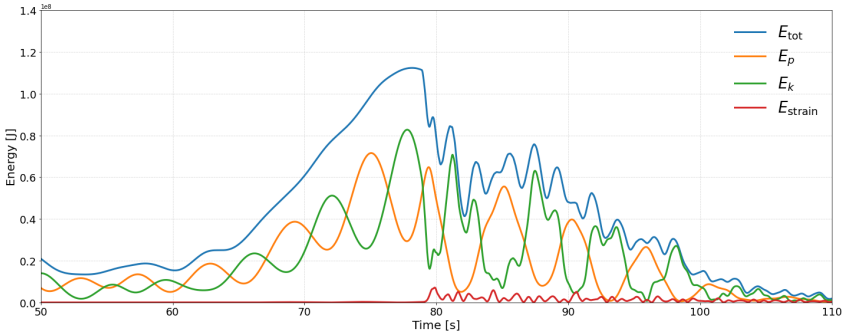

Figure 4.8: Energy response during the first impact for Case 3

During impact A clear distinction can be made between the pre-contact and post-contact phases of the response. During the initial free-floating stage, the total mechanical energy exhibits a relatively smooth and oscillatory behaviour, characteristic of wave-induced vessel motions governed primarily by hydrodynamic excitation and restoring forces. Following touchdown, the energy response becomes significantly more irregular, with increased fluctuations and intermittent peaks.

Figure 4.8 provides a closer view of the first touchdown event in case 3 and highlights the abrupt change in the energy response at the moment of contact. Prior to impact, the total mechanical energy varies smoothly, following the regular oscillatory pattern of the free-floating vessel motion. At the instant of first contact, this behaviour is interrupted by a sudden local disturbance in the energy signal. This transition occurs simultaneously with the first non-zero increase in the total strain energy E_{strain}, indicating that part of the vessel's mechanical energy is transferred into elastic deformation of the leg structure. The zoomed response also shows that the strain energy does not increase gradually, but appears as a short-duration peak associated with the impact event. This confirms that the touchdown introduces a transient energy exchange that is not present during the pre-contact phase. Although the magnitude of E_{strain} remains small compared with the global kinetic and potential energy components, its sudden appearance marks the onset of spudcan–seabed interaction and provides a direct indication of the internal structural response during impact.

Lifting During the lifting phase, the hull is gradually raised from its floating condition. This is visible in the plots as the strong increase in potential energy E_p after approximately 200 s. The increase is caused by the growing elevation of the vessel mass and should therefore not be interpreted as wave-induced energy build-up or as energy transferred through touchdown impact. It mainly represents external work introduced by the jacking system as the hull is raised relative to the legs.

The peaks that occur during this increase indicate that the lifting process is not completely smooth. While the potential energy rises steadily, intermittent contact and dynamic interaction between the spudcans and seabed cause short fluctuations in the energy response. These peaks are especially visible in Case 3, where the kinetic energy E_k and strain energy E_{strain} also show stronger irregular variations.

This jacking-system energy input is acknowledged in the present analysis, but it is not evaluated as a separate power contribution. The energy-based indicator analysis therefore focuses on the free-floating and impact response before and during touchdown, rather than on the later lifting-induced increase in potential energy.

4.2.3 Spudcan impact forces

Figure 4.9 shows the force response for the four spudcans during the same impact simulation.

The spudcans are numbered as follows:

- spudcan 1: starboard bow;
- spudcan 2: port bow;
- spudcan 3: starboard quarter;
- spudcan 4: port quarter.

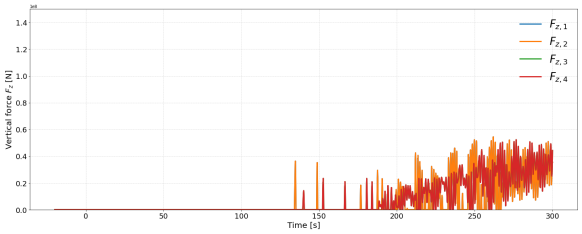

(a) Case 1

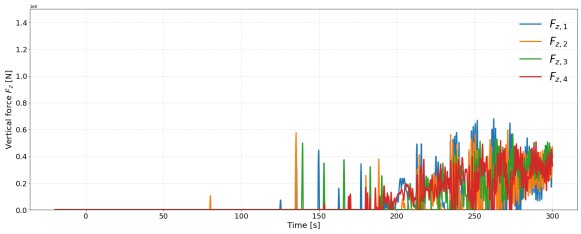

(b) Case 2

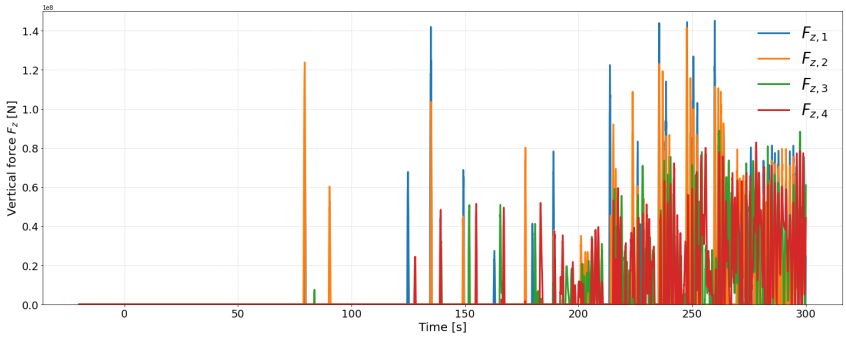

(c) Case 3

Figure 4.9: Vertical impact force response for Cases 1–3.

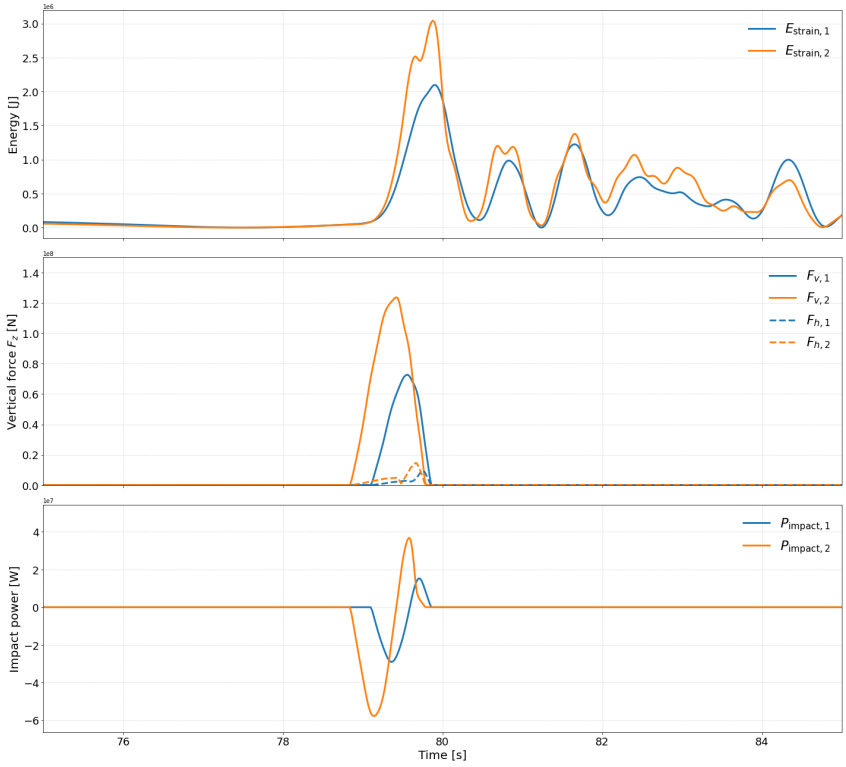

Figure 4.10: Impact response for Case 3: (a) strain energy per active leg, (b) vertical and horizontal impact forces at the corresponding spudcans, and (c) associated impact power.

Note that, due to the head wave condition in Case 1 and the resulting symmetric vessel response, the vertical impact forces over time are identical for spudcans 1 and 2, as well as for spudcans 3 and 4.

The impact force response confirms the interpretation obtained from the energy response. During the first part of the simulation, the impact forces remain zero. Shortly after the first impact, additional force peaks occur at the other spudcans, showing the sequence of intermittent contact events. The individual spudcans make contact with the seabed at different times, depending on the instantaneous vessel motion and orientation.

4.2.4 Energy exchange during spudcan impact

Zooming in on a touchdown event gives additional insight into the physical behaviour of the impact. Figure 4.10 shows the total strain energy, the vertical and horizontal impact forces at the active spudcans, and the corresponding impact power during the first impact events.

The impact power is determined according to the power balance term $P_{\text{imp}} = \mathbf{v}^T \mathbf{F}_{\text{imp}}$, the response shows that each touchdown event consists of a loading and unloading phase. In the plot, negative impact power indicates that energy is extracted from the global vessel motion and transferred into the contact system. This occurs during the initial loading phase of each impact, when the impact force rapidly increases. Shortly afterwards, the impact power becomes positive for a shorter interval, indicating that part of the temporarily stored energy is returned to the vessel during unloading. This behaviour is consistent with elastic recovery of the legs and the local impact response after compression.

However, the positive power contribution is smaller than the preceding negative contribution. Therefore, only part of the absorbed energy is returned to the system, and each impact event results in a net reduction of the global mechanical energy. The zoomed response therefore shows that spudcan touchdown is not only an intermittent force event, but also a transient energy-exchange process between vessel motion, leg deformation, and seabed contact.

4.3 Towards an energy-based response indicator

The results in this chapter show that the energy formulation provides a physically consistent description of the jack-up response in both the free-floating and impact simulations. In the free-floating simulation, the global mechanical energy represents the wave-induced motion response of the vessel. During impact, the same formulation remains applicable, while additional energy exchange occurs through spudcan contact, leg deformation and soil-spudcan interaction.

The results also confirm the strongly time-dependent character of the GoL response discussed earlier. Touchdown severity cannot be attributed to a single force, displacement or energy value, but depends on the instantaneous global motion state of the jack-up and its evolution around the moment of seabed contact. This motivates a closer evaluation of the global energy behaviour before and during touchdown. Since the energy response combines the translational and rotational motion of the vessel into a single mechanical quantity, it may reveal characteristic response patterns associated with more severe touchdown events.

An energy-based indicator could therefore provide an additional means to interpret why certain touchdown events become more critical than others. By identifying characteristic energy behaviour before or during contact, recurring response patterns associated with severe impacts

may be recognised. The following chapter therefore moves from individual response histories to a comparison across multiple simulations, evaluating whether the global energy response contains features related to touchdown severity.

Energy-based indicator 5

This chapter evaluates the energy-based indicators introduced in the methodology. First, the impact simulation results are used to assess whether the time-dependent energy response can explain transient touchdown severity. Within this analysis, same-seed no-impact simulations are used as reference responses to examine whether elevated-energy intervals occur during the touchdown window. The three-hour free-floating steady-state simulations are then used to assess whether characteristic energy quantities can support a pre-impact workability indicator.

5.1 GoL allowable case classification

The energy formulation is applied to cases that are classified as allowable limit cases, obtained using the framework by Holland and Hoogeveen (2023). As explained earlier, an allowable case is defined as a case with a unity check equal to 1.0, which means that the case lies exactly at the allowable capacity.

Unity checks are evaluated with respect to the following capacities:

- F_z: vertical spudcan force, resulting in axial loading of the pinions within the jacking system. The corresponding capacity is therefore governed by the allowable pinion force.
- $F_{x,y}$ in combination with F_z: horizontal and vertical spudcan forces, resulting in bending moments in the jack-up legs at the guides within the jacking system. The corresponding capacity is governed by the structural resistance of the leg chords and braces.

The unity check of a case is evaluated using a seed-based probabilistic approach, in which multiple wave realizations are simulated for each environmental condition. For every seed, the maximum response (F_z or $F_{x,y}$) is extracted, resulting in a distribution of peak responses across the considered realizations. The unity check assessment is subsequently based on the P90 value of this distribution, representing the response level exceeded by 10% of the simulated seeds. Figure 5.1 illustrates an example of such a seed variation for an environmental condition classified as allowable, showing the ordered maximum responses obtained for individual seeds and the corresponding P90 value used in the assessment.

5.2 Impact energy response under seed variation

This section first examines whether high-impact seeds are preceded by a common feature in the global mechanical energy response, such as a high energy level, a rising trend, or a clear pre-impact peak. The analysis examines whether energy-based metrics during the impact phase can help explain touchdown severity, as measured by touchdown loads and unity checks.

To examine this, an allowable case is selected as a representative environmental condition, corresponding to a sea state with significant wave height $H_s = 2.0$ m, peak period $T_p = 12$ s, and wave heading $\beta = 120°$. For this environmental condition, a seed variation study consisting

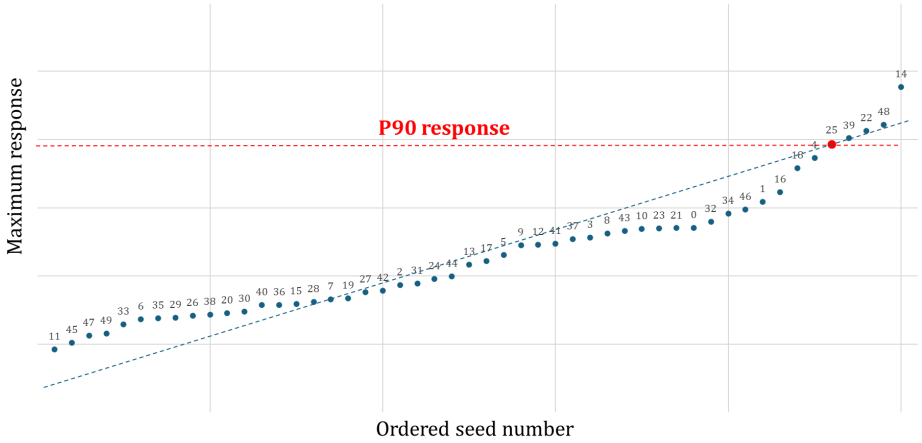

Figure 5.1: Illustration of the P90 determination procedure based on multiple wave seed realizations.

of 50 simulations is performed. The wave seeds are numbered from 0 to 49, and are ordered by response (Figure 5.1).

5.2.1 Energy behaviour prior and during impact

As shown in Figure 5.1, seeds 25, 39, 22, 48, and 14 exceed the allowable force capacity and therefore represent the five most critical cases within the analysed seed variations. These seeds are compared in Figure 5.2.

The following observations are made:

- A high value of E_{tot} before impact is not a common feature of all critical cases. Seed 22 shows relatively high energy levels before the largest impacts, whereas seeds 39 and 48 remain at more moderate energy levels while still exceeding the allowable force capacity.
- An increase in E_{tot} towards impact is also not consistently observed. In seed 25, E_{tot} generally decreases towards the maximum vertical impact force, while seed 14 shows a more gradual increase. Seed 25 shows a fluctuating response rather than a clear increasing or decreasing trend.
- A single clear energy peak before the critical force response cannot be identified for all cases. Seed 25 shows several fluctuations before the high-impact events, while seeds 39 and 48 show a less pronounced pre-impact energy response.
- All five seeds show a build-up of vertical impact forces over successive contact events, with the largest peak occurring near the end of the impact sequence. This could indicate a build-up of energy in the response, where later impacts occur under more critical conditions than the initial touchdown.
- The kinetic and potential energy components respond differently to impact events. Kinetic energy becomes more irregular during repeated impacts, as it depends directly on the instantaneous velocities of the hull and legs. Short contact, rebound, and deceleration events during touchdown therefore cause rapid changes in the kinetic energy response. In contrast, potential energy is mainly governed by the vertical position of the jack-up system, which changes more gradually during jacking. As a result, the potential energy

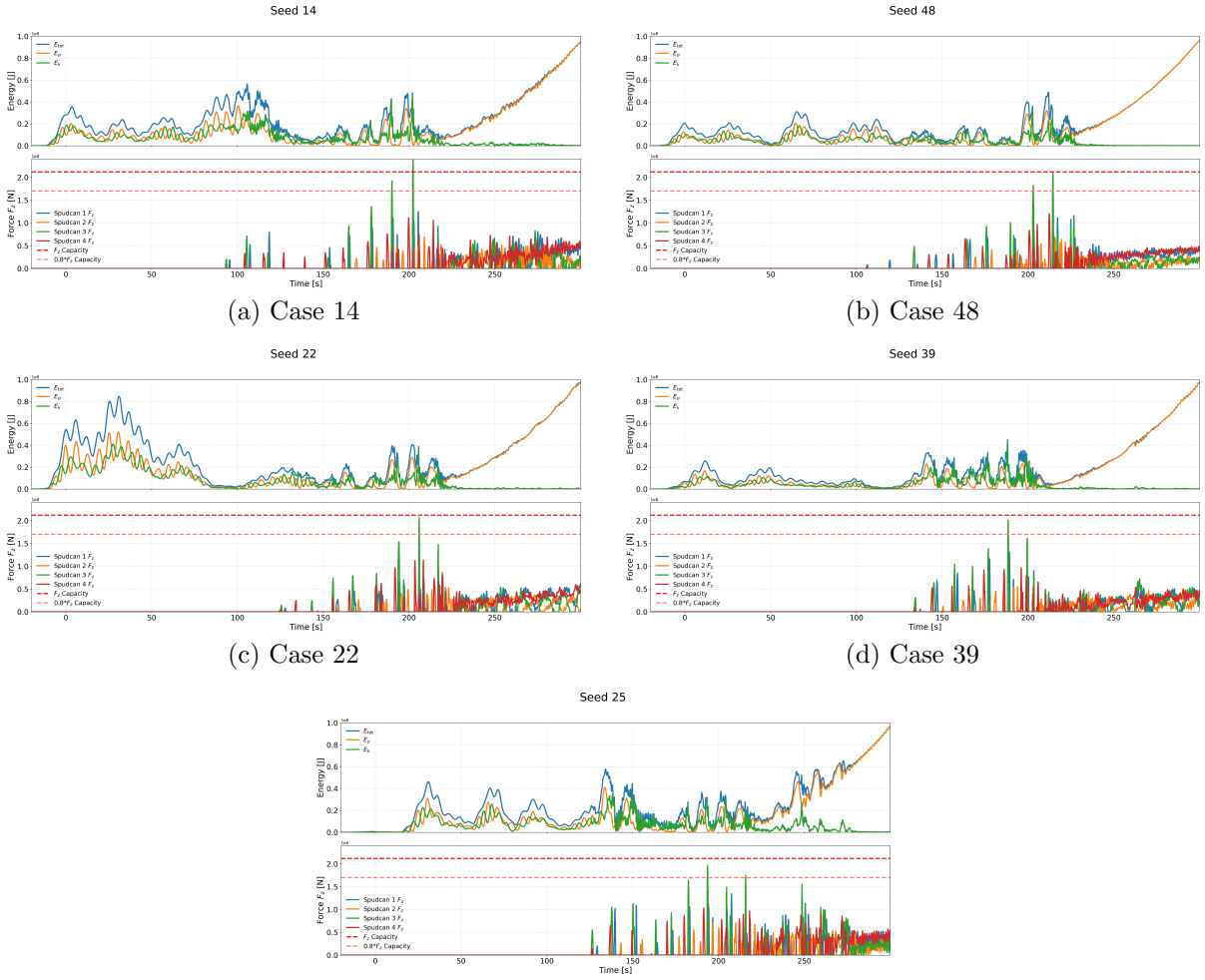

(a) Case 14

(b) Case 48

(c) Case 22

(d) Case 39

(e) Case 25

Figure 5.2: Energy response and impact force time series for selected cases.

remains smoother and follows the overall elevation trend.

These differences indicate that the critical seeds do not share a unique global energy signature before the largest force response. A high value of total energy, a rising energy trend, or a distinct pre-impact energy peak is therefore not a necessary condition for exceeding the force limit. Conversely, the repeated force build-up visible in all critical seeds suggests that the final peak force is governed by the contact sequence and the instantaneous touchdown conditions, rather than by the pre-impact global energy level alone.

5.2.2 Energy response of impact-disabled simulations

The impact simulations from section 5.2.1 are compared with impact-disabled reference simulations. These are referred to as same-seed no-impact simulations in the remainder of this section. A same-seed no-impact simulation uses the same environmental condition and wave realisation as the corresponding impact simulation, but with soil-spudcan interaction disabled. The resulting response therefore represents how the vessel would move under the same wave realisation without interruption by spudcan-seabed contact.

Figure 5.3 compares seeds 18, 39, 40, and 44. The comparison is used to examine whether elevated intervals in the undisturbed vessel-energy response coincide with the touchdown window in the corresponding impact simulation.

The following observations are made:

- Seeds 18 and 39 show a clear interval of elevated energy in the no-impact response around the period where the main impacts occur in the impact simulation. This means that, for these seeds, the touchdown phase coincides with a relatively energetic part of the no-impact vessel response.
- A similar elevated-energy interval is also visible in the impact response. Around the main impact phase, E_{tot} tends to increase, consistent with the elevated-energy interval observed in the no-impact simulation. However, once touchdown occurs, the energy response is interrupted by the impact. As a result, the increase in E_{tot} does not continue smoothly, but is followed by drops and fluctuations during the repeated impact events. The fact that E_{tot} repeatedly tends to increase between successive impacts indicates that the vessel remains within an energetic response interval during this phase. This helps explain why the impact forces can build up over multiple contact events, rather than being governed by a single isolated energy peak.
- Seeds 40 and 44 also contain energy peaks in the no-impact response, but these peaks do not coincide as strongly with severe spudcan impacts. In seed 40, the largest no-impact energy peak occurs before the main impact phase. In seed 44, the no-impact response contains several peaks, but the impact forces remain relatively low.

The comparison shows that the relevance of energy in the no-impact response depends on its timing relative to touchdown. A pronounced elevated-energy interval in the no-impact response is not critical by itself. It becomes relevant when it occurs during the touchdown window, because the vessel is then in an energetic motion state while the spudcans are close enough to interact with the seabed.

Overall, these results indicate that the no-impact response provides useful information about impact severity mainly when it is evaluated relative to the expected touchdown window.

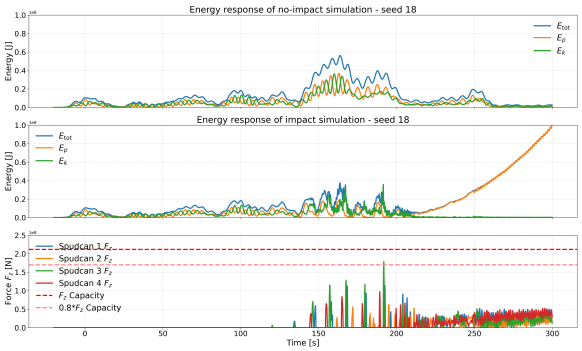

(a) Seed 18

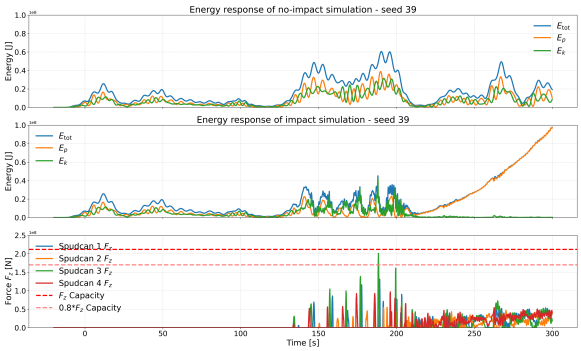

(b) Seed 39

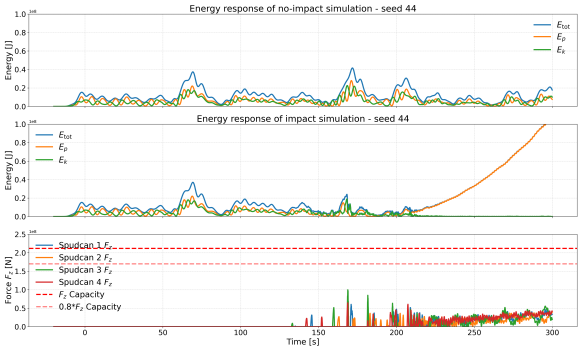

(c) Seed 44

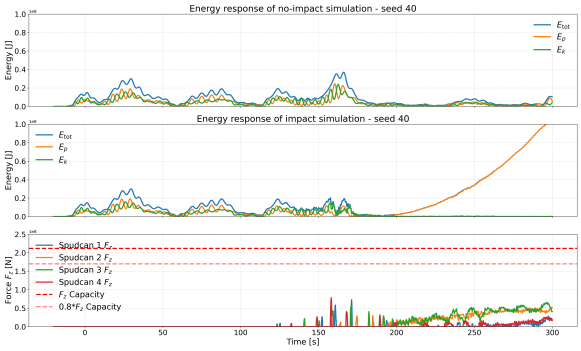

(d) Seed 40

Figure 5.3: Comparison between no-impact and impact response for selected wave seeds.

5.2.3 Energy-response groups and touchdown-window timing

In this thesis, an energy-response group is defined as a time interval in the no-impact or free-floating energy response during which the global mechanical energy remains elevated over several wave cycles. It represents a grouped response feature of the vessel motion, rather than a single instantaneous energy peak.

The comparison between the same-seed no-impact and impact simulations suggests that the relevance of such groups depends on their overlap with the touchdown window. The selected severe-impact cases are associated with elevated intervals in the no-impact energy response that coincide with the phase in which the spudcans are close enough to the seabed to generate impact forces. In contrast, large no-impact energy peaks are not necessarily critical when they occur outside this window, while more moderate energy levels may still lead to severe forces when they occur during touchdown.

This shows that the energy response is not relevant only through its absolute magnitude. Its relevance also depends on whether the vessel is in an energetic motion state while spudcan-seabed interaction can occur. An energy-response group should therefore not be interpreted as directly determining the impact force, but as indicating a time interval in which the vessel response may become more critical if touchdown takes place.

5.3 Free-floating steady-state energy response

The free-floating steady-state simulations are used to assess whether allowable limit cases exhibit a consistent steady-state energy response that could support a pre-impact workability indicator. Following the same-seed comparison, they are also used to examine whether similar elevated-energy intervals occur over a longer operational time window. These intervals are interpreted as energy-response groups and are subsequently counted and quantified using characteristic energy response measures.

5.3.1 Energy-response group detection

A simulation duration of three hours is adopted for the free-floating assessment to obtain a statistically representative steady-state response. This duration is consistent with offshore practice, where a sea state is commonly assumed to remain stationary over a three-hour period, to reduce the influence of transient behaviour and phase-dependent variability (Det Norske Veritas, 2011).

The considered case numbers and corresponding sea states (on the same set of seeds) used in the free-floating assessment are presented in Table 5.1 and Table 5.2, respectively.

		Peak period (s)				
		10	12	14	16	18
Direction (deg)	0	0	1	2	3	4
	30	5	6	7	8	9
	60	10	11	12	13	14
	90	15	16	17	18	19
	120	20	21	22	23	24
	150	25	26	27	28	29
	180	30	31	32	33	34

Table 5.1: Case numbering of sea states

		Peak period (s)				
		10	12	14	16	18
Direction (deg)	0	5.1	3.1	2.7	2.6	2.8
	30	4.0	2.9	2.6	2.3	2.7
	60	2.4	2.3	2.1	2.1	2.1
	90	1.9	1.8	1.7	1.7	1.8
	120	2.2	2.0	1.9	1.8	1.9
	150	3.6	2.8	2.5	2.2	2.4
	180	4.8	3.4	2.8	2.8	2.7

Table 5.2: Allowable significant wave height (m) per sea state

The first 1000 seconds of cases 02, 26 and 34, shown in Figure 5.4, illustrate that the free-floating response is not a single steady energy level. Instead, the response consists of repeated energy-response groups. These groups differ in magnitude, duration and persistence between cases, even when the cases have the same significant wave height. This shows that the three-hour free-floating response contains interval-based information about when the vessel motion becomes more energetic. The complete three-hour energy responses for all cases are provided in Appendix D.

Because these energy-response groups vary between sea states, both their occurrence and their characteristic energy level must be quantified before the free-floating response can be compared systematically. The following section therefore defines characteristic energy response measures that describe both the maximum response and the more persistent energetic part of the response.

5.3.2 Definition of characteristic energy response measures

For each three-hour simulation, the time series of the total energy E_{tot}, kinetic energy E_k and potential energy E_p are evaluated. In addition, the time derivative of the total energy, $\frac{dE_{\text{tot}}}{dt}$, is considered in order to describe the rate at which energy is transferred during the response.

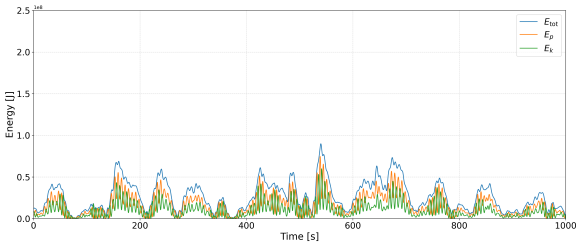

(a) Case 02

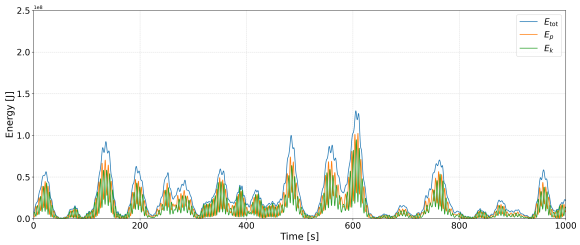

(b) Case 26

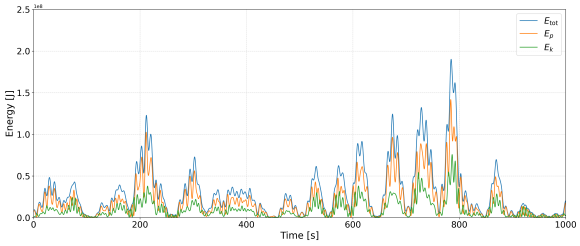

(c) Case 34

Figure 5.4: Comparison of the first 1000 seconds of the three-hour free-floating energy response for selected cases.

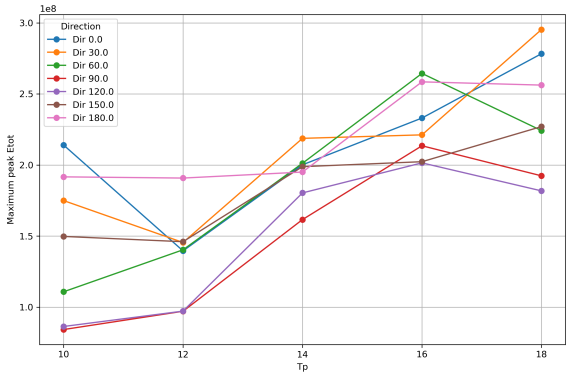

(a) Maximum total energy $E_{\mathrm{tot,max}}$

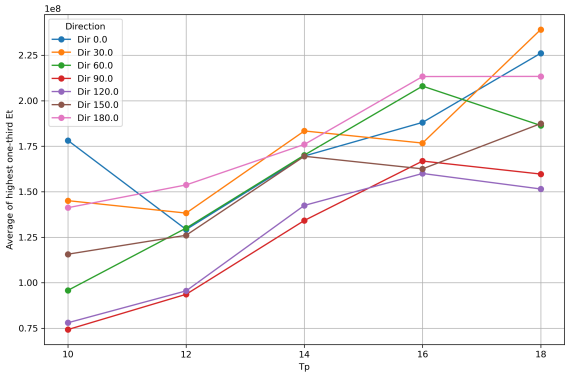

(b) Significant total energy $E_{\mathrm{tot},1/3}$

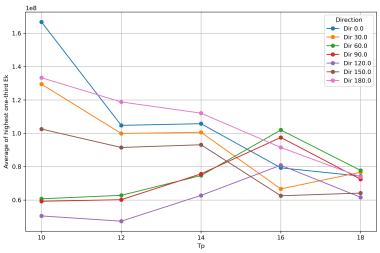

(c) Kinetic energy $E_{\mathrm{k},1/3}$

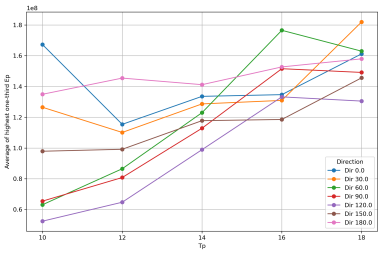

(d) Potential energy $E_{\mathrm{p},1/3}$

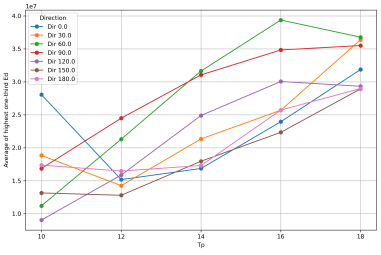

(e) Energy rate $\left(\frac{\mathrm{d}E}{\mathrm{d}t}\right)_{1/3}$

Figure 5.5: Summary of free-floating energy responses.

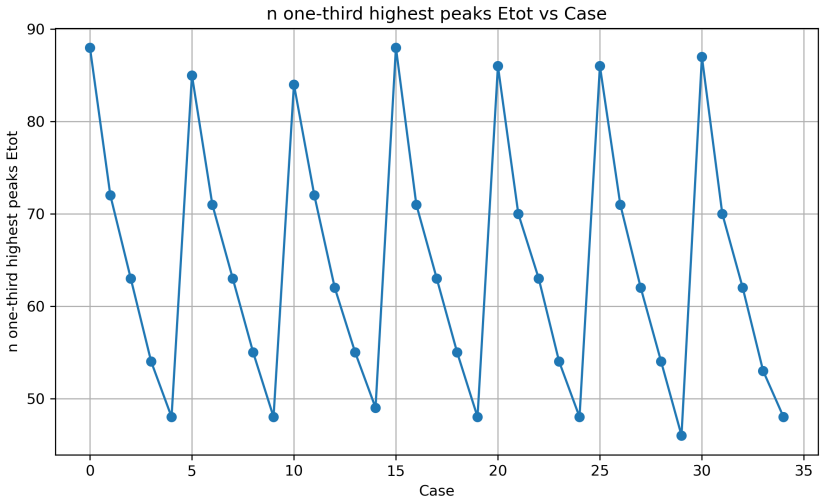

Figure 5.6: $N_{1/3}$ highest peaks of E_{tot} according to the case number in Table 5.1

For each quantity, characteristic values are derived using two different interpretations: a maximum-response approach and a statistical significant-response approach. The maximum-response approach considers the largest positive value observed during the three-hour simulation. For a generic energy-related quantity $X(t)$, this value is defined as:

$$X_{\max} = \max_{t} X(t) \tag{5.1}$$

where $X(t)$ may represent E_{tot}, E_k, E_p or $\frac{dE_{\text{tot}}}{dt}$. The maximum value represents the largest positive instantaneous response observed in the simulation. $X_{\max}$ is interpreted as the governing worst-case value for that specific simulation. This measure is conservative, but it is also sensitive to a single extreme peak in the time trace.

A second characteristic value is defined using a statistical significant-response approach, aimed at identifying energy-response groups in the free-floating response. Instead of relying on a single maximum value, this approach considers the upper part of the distribution of energy-response groups. Local positive maxima are first identified in the time series of the considered energy-related quantity. To avoid selecting multiple peaks that belong to the same energy-response group, a minimum separation distance is imposed between consecutive peaks. This distance is defined proportional to the peak wave period, such that

$$\Delta t_{\text{peak}} = n_p T_p,$$

where T_p is the peak period of the sea state and n_p is a dimensionless peak separation factor. Scaling the peak distance with T_p ensures that the peak-selection procedure adapts to the dominant time scale of each sea state, rather than using a fixed time interval for all environmental conditions.

The value of n_p was determined from a sensitivity study in which different peak-distance factors were compared based on the consistency of numbers of identified peaks across the simulations. From this comparison, $n_p = 5$ was found to provide the most robust separation between individual energy-response group events and local fluctuations. Figure 5.6 shows the number of

identified upper-third energy peaks for each case using $n_p = 5$. The results show a consistent variation for cases with the same wave direction and peak period, indicating that this peak-distance criterion provides a stable separation between individual energy-response group events and local fluctuations. This value is therefore adopted in the present analysis.

After the peak detection step, the highest one-third of the identified peaks is selected. This upper-third subset is used to characterize the more energetic part of the response, while reducing the influence of smaller local fluctuations. The number of peaks in this subset can be interpreted as an indication of the number of more severe energy events or energy-response groups within the three-hour simulation.

From the identified peaks, the highest one-third values are selected and averaged, which results in a significant energy level, defined as:

$$X_{1/3} = \frac{1}{N_{1/3}} \sum_{i=1}^{N_{1/3}} X_{\text{peak},i}$$

where $X_{\text{peak},i}$ represents the positive local maxima belonging to the highest one-third of all identified positive peaks, and $N_{1/3}$ is the number of peaks included in this upper-third subset. When the considered quantity is the total energy, this value is denoted as $E_{\text{tot},1/3}$; similar definitions are used for E_k, E_p and $\frac{dE_{\text{tot}}}{dt}$.

5.3.3 Variation of characteristic energy response measures

The variation of the maximum and significant energy levels is shown in Figure 5.5 for all considered sea states. The responses do not vary uniformly with either peak period or wave direction. Instead, the trends differ per direction and per energy quantity.

The energy trends show that the relative contribution of potential energy increases with peak period, T_p. The kinetic energy, $E_{k,1/3}$, generally decreases or remains limited for increasing T_p, whereas the potential energy, $E_{p,1/3}$, shows a clearer increasing trend for most wave directions. This distinction is important for impact interpretation, because a high total mechanical energy level does not necessarily imply high impact potential when the response is mainly displacement-dominated. For touchdown severity, velocity-related quantities such as kinetic energy, energy rate, or local spudcan closing velocity may be more directly relevant.

The increase in significant total energy, $E_{\text{tot},1/3}$, at higher T_p is therefore mainly driven by potential energy rather than kinetic energy. This indicates that longer-period sea states are more dominated by displacement-related energy, while the relative importance of velocity-dependent kinetic energy decreases.

These results show that the free-floating steady-state response can be used to identify and characterise energy-response groups, but the characteristic energy quantities do not provide a consistent threshold or uniform separation between allowable and non-allowable cases. The variation between sea states depends on wave direction, peak period, and on the relative contribution of kinetic and potential energy. As a result, the free-floating energy response is useful for identifying energetic response intervals, but it cannot be used as a standalone workability criterion.

5.4 Main findings and implications

This chapter analysed the energy response of impact and free-floating simulations to evaluate its relation to touchdown severity during GoL.

The seed-variation analysis shows that the transient total energy response alone does not directly predict touchdown impact severity. Critical seeds do not share a consistent pre-impact energy level, energy trend, or distinct energy peak before the largest force response occurs. Therefore, the maximum impact force cannot be predicted from the global energy history alone. Instead, the impact response depends on the instantaneous combination of vessel motion, wave phase, spudcan-seabed clearance, and contact conditions at the moment of touchdown. However, the comparison does show that timing is important. Severe impacts mainly occur when an energetic part of the vessel response coincides with the touchdown window. This means that the global energy response is not a standalone force predictor, but it can help identify energy-response groups that become relevant when touchdown occurs during these intervals.

This role of energy-response group timing is also supported by the case-variation study. The total-energy analysis can be used to identify energy-response groups and to assess their relative severity within individual free-floating simulations. Peaks in the characteristic free-floating energy response indicate periods in which the vessel experiences more energetic motion, and therefore provide insight into potentially severe energy-response group events.

Overall, global mechanical energy should not be interpreted as a standalone workability criterion for GoL. The main value of the energy-based approach is that it shows the importance of timing between energy-response groups and spudcan-seabed interaction. Future work should therefore focus on three-hour simulations in a near-touchdown or initial-contact configuration, where the relation between local energy transfer, contact work, and impact magnitude can be evaluated more directly. This is further discussed in the next chapter.

Conclusion and Recommendations 6

This chapter presents the conclusions and recommendations of this study. The objective of the research was to investigate to what extent the global mechanical energy response of a jack-up vessel can be used as an indicator for touchdown severity and GoL workability assessment. To address this objective, the energy response was evaluated using impact simulations, same-seed no-impact simulations, and free-floating steady-state simulations.

The chapter first answers the research questions by focusing on the contribution of the energy-based method and on the extent to which it supports the interpretation of touchdown severity and GoL workability. The limitations section then addresses the aspects for which the energy-based approach was not sufficient.

6.1 Answer to the research questions

This section answers the main research question and the two sub-questions by summarizing the main findings.

RQ1: To what extent can the time-dependent energy response during the impact phase be used as an indicator for transient touchdown severity?

The seed-variation analysis shows that the time-dependent energy response can be used as a physically interpretable indicator for transient touchdown severity. By comparing impact simulations with same-seed no-impact simulations, energy-response groups are identified in the no-impact response. These groups represent intervals in which the vessel would be in an energetic motion state under the same wave realisation without seabed contact. Severe touchdown events are more likely when these intervals coincide with the touchdown window. The energy response therefore helps interpret when severe touchdown behaviour may develop, but does not directly predict the maximum impact force.

RQ2: To what extent can steady-state free-floating energy quantities provide an indication of allowable and non-allowable GoL cases?

The three-hour free-floating simulations show that the steady-state global energy response provides information about the occurrence and characteristics of elevated-energy intervals in the vessel response. Within this response, energy-response groups can be identified and characterised in terms of their magnitude, duration, development, and occurrence in time.

In this interval-based sense, the steady-state free-floating energy response can provide an indication of potentially severe vessel-motion states. However, the characteristic energy quantities considered in this study did not provide a consistent threshold or uniform separation between allowable and non-allowable GoL cases. The free-floating energy response is therefore useful for identifying energetic response intervals, but not as a standalone workability criterion.

Main RQ: To what extent can the global mechanical energy response of a jack-up vessel be used as a physically interpretable indicator for touchdown severity and GoL workability assessment?

Based on the findings of RQ1 and RQ2, the global mechanical energy response can be used as a physically interpretable measure for touchdown severity and GoL workability assessment. Its main contribution is that it links energetic vessel-motion states to the timing of touchdown events. The energy response should not be interpreted as a standalone workability criterion, because the final impact severity still depends on the local contact conditions and structural response. However, it provides a useful additional assessment layer by identifying and interpreting potentially critical vessel-response intervals before or during touchdown. With further calibration of energy-response-group characteristics, the global mechanical energy response could support more targeted impact simulations and more efficient screening of GoL conditions.

6.2 Limitations of the energy-based approach

Although the energy-based approach provides a physically interpretable measure of the vessel response during GoL, the results of this thesis also show clear limitations.

6.2.1 Limitations of the research-question outcomes

The seed-variation analysis shows that the time-dependent global energy response cannot be used as a direct predictor of impact-load magnitude. Critical seeds do not share a consistent pre-impact energy level, energy trend, or distinct energy peak before the largest force response occurs. Similar impact severity can therefore occur from different global energy histories. This limits the extent to which the impact energy response can be used to directly estimate the maximum impact force.

A similar limitation was found for the steady-state free-floating analysis. The three-hour free-floating energy response provides information about the occurrence and characteristics of energy-response groups, but the characteristic energy quantities considered in this study did not provide a uniform separation between allowable and non-allowable GoL cases. No consistent threshold or trend was found that could directly distinguish between the two classifications. This limits the use of the free-floating energy response as a standalone workability criterion.

6.2.2 Loss of local contact information

A limitation of the global-energy description is that the peak impact force is governed by the instantaneous local contact conditions at the moment of touchdown. These include the vessel position and orientation, spudcan velocity, spudcan-seabed clearance, wave phase, leg configuration, and possible previous contact events. The global energy response can indicate when the vessel is in an energetic motion state, but it does not contain enough local information to determine how that energy is transferred into a specific spudcan impact.

A second limitation is that the coupled GoL response is reduced to a single global energy quantity. The full touchdown process consists of several interacting mechanisms, including vessel motion, spudcan-seabed interaction, leg deformation, impact forces, and structural response, as explained in Section 2.1.2. Combining part of this response into one total energy measure, E_{tot}, provides a compact description of the global system response, but it also removes information that is important for interpreting local touchdown severity.

This is especially relevant for touchdown events involving multiple spudcans. A single global energy quantity cannot distinguish how much of the response is associated with one spudcan impact when two or more spudcans interact with the seabed during the same interval. As a result, similar values of E_{tot} may correspond to different local impact mechanisms and different force responses. The advantage of using one compact energy quantity therefore also becomes a limitation when the governing response is controlled by local contact behaviour.

6.3 Recommendations for future work

The findings of this thesis show that the global mechanical energy response is most useful when interpreted through the timing of energy-response groups relative to the touchdown window. Future work framework should be built in two sequential steps. First, fixed-configuration impact simulations should be used to determine which energy-response-group characteristics are associated with severe touchdown behaviour. Second, once these critical characteristics are known, future work should investigate whether they can be detected more efficiently in the free-floating response using frequency-domain or reconstructed energy-response quantities.

6.3.1 Calibration using fixed-configuration impact simulations

The first recommendation is to use fixed-configuration impact simulations to study the relation between energy-response groups and touchdown severity in a controlled setting. Long-duration no-impact simulations can first be used to provide the undisturbed vessel-energy response over a full sea-state realisation. Controlled impact simulations can then be performed for selected parts of this response, using a prescribed leg configuration and initial spudcan-seabed clearance. This approach can help isolate the effect of the instantaneous conditions by reducing the variability of the touchdown configuration.

The calibration should start from the impact response. For a fixed touchdown configuration, the highest impact events can first be identified from the spudcan force time series. The corresponding intervals in the same-seed no-impact energy response can then be examined to determine whether these impacts occur during an energy-response group. Each associated group can be characterised by quantities such as total energy level, duration, rate of energy increase, timing relative to touchdown, vertical velocity, and spudcan-seabed clearance.

In this way, fixed-configuration simulations can provide the physical link between the global energy-response group and the local touchdown mechanism that determines the final impact force.

6.3.2 RAO-based reconstruction for probabilistic screening

The second recommendation is to investigate whether the free-floating energy response can be reconstructed using RAOs and the wave spectrum. Once the relevant energy-response-group characteristics have been calibrated using fixed-configuration impact simulations, an RAO-based approach could be used to identify similar groups without running a separate three-hour time-domain simulation for every wave realisation.

The reconstructed response could then be used to evaluate the statistical occurrence of potentially critical energy-response groups within a sea state. Instead of assessing only one simulated realisation, multiple realisations could be generated from the same spectral description. This

would make it possible to estimate the probability that the free-floating vessel response contains energy-response groups with characteristics associated with severe touchdown behaviour.

In this way, the RAO-based reconstruction would extend the energy-based approach from time-domain interpretation toward efficient screening. The objective would not be to predict the impact force directly, but to estimate how likely it is that a sea state contains energetic response intervals that may become critical if touchdown occurs during those intervals.

References

Cassidy, M. J., & Houlsby, G. T. (1999). On the modelling of foundations for jack-up units on sand. *Offshore Technology Conference*, (10995).

Chakrabarti, P. (2012). Going on location study for a jack-up rig. *Proceedings of the ASME 31st International Conference on Ocean, Offshore and Arctic Engineering*.

Chopra, A. K. (2020). *Dynamics of structures: Theory and applications to earthquake engineering* (5th). Pearson Education Limited.

Daun, V., & Olsson, F. (2014). *Impact loads on a self-elevating unit during jacking operation: A methodology incorporating site-specific parameters for weather window assessment* (Publication No. 2014:X-14/299) [Master's Thesis]. Chalmers University of Technology.

Det Norske Veritas. (2011, April). *DNV-RP-H103: Modelling and Analysis of Marine Operations* (Recommended Practice No. DNV-RP-H103) (Accessed: 2026-05-21). Det Norske Veritas. Høvik, Norway. https://home.hvl.no/ansatte/gste/ftp/MarinLab_files/Litteratur/DNV/rp-h103_2011-04.pdf

DNV. (2022). *Self-elevating units* (Recommended Practice No. DNV-RP-C104). DNV. Høvik, Norway.

European Commission. (2024). The European Green Deal.

Fang, Y.-S., Liu, C., Chen, S.-L., & Shih, Y.-C. (2019). Penetration resistance of jack-up spudcan on dense sand overlying loose sand. *Journal of GeoEngineering*, *14*(3), 129–139. https://doi.org/10.6310/jog.201909_14(3).2

Fossen, T. I. (2021). *Handbook of marine craft hydrodynamics and motion control* (2nd ed.). John Wiley & Sons.

Fossen, T. I. (2025). Maneuvering coefficient estimation from frequency-dependent added mass and damping: A power-based approach. *Ocean Engineering*, *341*, 122494. https://doi.org/10.1016/j.oceaneng.2025.122494

Goldsmith, W. (1960). *Impact: The theory and physical behaviour of colliding solids*. Edward Arnold (Publishers) Ltd.

Green, E. (2024). *Unprecedented collapse in eu coal and gas electricity generation last year, report reveals*. Euronews. Retrieved February 6, 2026, from https://www.euronews.com/green/2024/02/07/unprecedented-collapse-in-eu-coal-and-gas-electricity-generation-last-year-report-reveals

Guachamin Acero, W., Li, L., Gao, Z., & Moan, T. (2016). Methodology for assessment of the operational limits and operability of marine operations. *Ocean Engineering*, *125*, 308–327. https://doi.org/10.1016/j.oceaneng.2016.08.015

Guyan, R. J. (1965). Reduction of stiffness and mass matrices. *AIAA Journal*, *3*(2), 380. https://doi.org/10.2514/3.2874

Hibbeler, R. C. (2016a). *Engineering mechanics: Dynamics* (14th ed.). Pearson.

Hibbeler, R. C. (2016b). *Mechanics of materials* (10th ed.). Pearson.

Holland, G. F., & Hoogeveen, S. M. (2023). Going-on-location of jack-ups: A comprehensive framework for site-specific assessment of installation [Conference paper].

Hu, P., Haghighi, A., Coronado, J., Leo, C., Liyanapathirana, S., & Li, Z. (2021). A comparison of jack-up spudcan penetration predictions and recorded field data. *Applied Ocean Research*, *112*, 102713. https://doi.org/10.1016/j.apor.2021.102713

Identec Solutions. (2024). *The essential role of windfarm support vessels*. Identec Solutions. Retrieved February 6, 2026, from https://www.identecsolutions.com/news/the-essential-role-of-windfarm-support-vessels

Izadi, E., & Vazquez, J. H. (2023). Wtiv touch-down loads on hard seabeds. *Offshore Technology Conference*.

Journée, J. M. J., & Massie, W. W. (2008). *Offshore hydromechanics* (2nd ed.). Delft University of Technology.

Le, C.-h., Li, Y.-e., Huang, L., Ren, J.-y., Ding, H.-y., & Zhang, P.-y. (2021). Collision analysis between spudcan and seabed during the process of jack-up platform lowering jack-up legs. *China Ocean Engineering*, *35*(5), 779–788. https://doi.org/10.1007/s13344-021-0069-1

Lee, J., & Randolph, M. (2010). Penetrometer-based assessment of spudcan penetration resistance. *Journal of Geotechnical and Geoenvironmental Engineering*, *137*(6), 587–596. https://doi.org/10.1061/(ASCE)GT.1943-5606.0000453

Lynch, K. M., & Park, F. C. (2017). *Modern robotics: Mechanics, planning, and control* [Preprint available online]. Cambridge University Press. http://hades.mech.northwestern.edu/images/2/2e/MR-largefont-v2.pdf

Matter, G. B., da Silva, R. R. M., & Tan, P.-L. (2005). Touchdown analysis of jack-up units for the definition of the installation and retrieval operational limits. *Proceedings of the 24th International Conference on Offshore Mechanics and Arctic Engineering (OMAE2005)*.

Miller, B. L., Frieze, P. A., Lai, P. S. K., Lewis, T. C., & Smith, I. A. A. (1993). Motion and impact responses of jackups moving onto location. *Offshore Technology Conference*, (7301).

Orcina Ltd. (2025a). *Orcaflex help: Online documentation*. https://www.orcina.com/webhelp/OrcaFlex/

Orcina Ltd. (2025b). *Orcawave help: Online documentation*. https://www.orcina.com/webhelp/OrcaWave/

Rao, K. R. (2016). *Applied impact mechanics*. Wiley.

Rao, S. S. (2017). *Mechanical vibrations* (6th ed.). Pearson.

Ringsberg, J. W., Daun, V., & Olsson, F. (2017). Analysis of impact loads on a self-elevating unit during jacking operation. *Journal of Offshore Mechanics and Arctic Engineering*, *139*(3), 031602. https://doi.org/10.1115/1.4035996

Smith, I. A. A., Frieze, P. A., Lai, P. S. K., Lewis, T. C., & Miller, B. L. (1994). Evaluation of leg damage risk for jack-ups going on location. *Proceedings of the Offshore Technology Conference*, (7530).

Smith, I. A. A., Lai, P. S. K., Lewis, T. C., & Miller, B. L. (1995). Limiting motions for jack-ups moving onto location [Technical paper on jack-up touchdown limiting motions]. *Global Maritime / Paul A. Frieze & Associates report*.

Spidsoe, N., & Karunakaran, D. (1996). Nonlinear dynamic behaviour of jack-up platforms. *Marine Structures*, *9*(1), 71–100. https://doi.org/10.1016/0951-8339(95)00005-4

SWZ Maritime. (2022, September 16). *Jan de nul installs eighty turbines at first french offshore wind farm*. Retrieved February 26, 2026, from https://swzmaritime.nl/news/2022/09/16/jan-de-nul-installs-eighty-turbines-at-first-french-offshore-wind-farm/

Vazquez, J. H., Grasso, B. D., Gamino, M., & III, J. S. T. (2017). Seabed modeling effects on jack-up response while going on location. *Proceedings of the ASME 36th International Conference on Ocean, Offshore and Arctic Engineering (OMAE2017)*.

Vazquez, J. H., Grasso, B. D., Gamino, M. A., & Wang, W. (2016). Jackups going on location: Understanding energy principles on leg impact loads. *Proceedings of the 21st Offshore Symposium*.

Vazquez, J. H., Michel, R. P., Alford, J. H., Quah, M., & Foo, K. S. (2005). *Jack up units: A technical primer for the offshore industry professional* [Updated July 1, 2005]. Bennett & Associates, L.L.C. and Offshore Technology Development Inc. New Orleans, LA, Singapore. http://www.bbengr.com

Williams, M. S., Thompson, R. S. G., & Houlsby, G. T. (1998). Non-linear dynamic analysis of offshore jack-up units. *Computers and Structures*, *69*, 171–180. https://doi.org/10.1016/S0045-7949(98)00119-9

A Derivation of the adjoint transformation matrix

Starting from the cross product

$$\mathbf{r} \times \mathbf{F} = \begin{bmatrix} x \\ y \\ z \end{bmatrix} \times \begin{bmatrix} F_x \\ F_y \\ F_z \end{bmatrix} = \begin{bmatrix} yF_z - zF_y \\ zF_x - xF_z \\ xF_y - yF_x \end{bmatrix}, \tag{A.1}$$

this can be written in matrix form as

$$\mathbf{r} \times \mathbf{F} = [\mathbf{r}]_\times \mathbf{F}, \tag{A.2}$$

with the skew-symmetric matrix

$$[\mathbf{r}]_\times = \begin{bmatrix} 0 & -z & y \\ z & 0 & -x \\ -y & x & 0 \end{bmatrix}. \tag{A.3}$$

Using the moment shift relation

$$\mathbf{M}_{COG} = \mathbf{M}_L - \mathbf{r} \times \mathbf{F}_L, \tag{A.4}$$

the translation from the local reference point to the COG becomes

$$\begin{bmatrix} \mathbf{F}_{COG} \\ \mathbf{M}_{COG} \end{bmatrix} = \begin{bmatrix} \mathbf{I}_3 & \mathbf{0} \\ -[\mathbf{r}]_\times & \mathbf{I}_3 \end{bmatrix} \begin{bmatrix} \mathbf{F}_L \\ \mathbf{M}_L \end{bmatrix}. \tag{A.5}$$

The rotation from the local body-fixed frame to the global frame is constructed from roll, pitch, and yaw as

$$\mathbf{R} = \mathbf{R}_{\text{yaw}}\, \mathbf{R}_{\text{pitch}}\, \mathbf{R}_{\text{roll}}, \tag{A.6}$$

with

$$\mathbf{R}_{\text{roll}} = \begin{bmatrix} 1 & 0 & 0 \\ 0 & \cos\phi & -\sin\phi \\ 0 & \sin\phi & \cos\phi \end{bmatrix}, \qquad \mathbf{R}_{\text{pitch}} = \begin{bmatrix} \cos\theta & 0 & \sin\theta \\ 0 & 1 & 0 \\ -\sin\theta & 0 & \cos\theta \end{bmatrix}, \tag{A.7}$$

$$\mathbf{R}_{\text{yaw}} = \begin{bmatrix} \cos\psi & -\sin\psi & 0 \\ \sin\psi & \cos\psi & 0 \\ 0 & 0 & 1 \end{bmatrix}. \tag{A.8}$$

Hence,

$$\begin{bmatrix} \mathbf{F}_G \\ \mathbf{M}_G \end{bmatrix} = \begin{bmatrix} \mathbf{R} & \mathbf{0} \\ \mathbf{0} & \mathbf{R} \end{bmatrix} \begin{bmatrix} \mathbf{F}_{COG} \\ \mathbf{M}_{COG} \end{bmatrix}. \tag{A.9}$$

Combining translation and rotation gives the final 6×6 matrix:

$$\begin{bmatrix} \mathbf{F}_G \\ \mathbf{M}_G \end{bmatrix} = \begin{bmatrix} \mathbf{R} & \mathbf{0} \\ -\mathbf{R}[\mathbf{r}]_\times & \mathbf{R} \end{bmatrix} \begin{bmatrix} \mathbf{F}_L \\ \mathbf{M}_L \end{bmatrix}. \tag{A.10}$$

Thus, the complete transformation matrix is

$$\mathbf{T} = \begin{bmatrix} \mathbf{R} & \mathbf{0} \\ -\mathbf{R}[\mathbf{r}]_\times & \mathbf{R} \end{bmatrix} \tag{A.11}$$

B Mass matrix calculation for free-floating and impact configuration

This appendix describes the calculation framework used to obtain the mass properties for the jack-up vessel in the legs-down impact condition. The transformation starts from the free-floating legs-up condition and modifies the mass and inertia properties to represent the legs-down configuration used in the impact simulations.

The calculation distinguishes between the following configurations:

- **Situation A:** contribution of the legs in the raised position;
- **Situation B:** complete vessel with legs up, representing the free-floating condition;
- **Situation C:** contribution of the legs in the lowered position;
- **Situation D:** complete vessel with legs down, representing the impact condition.

The legs-down impact condition is obtained by removing the legs-up contribution from the free-floating vessel and adding the legs-down contribution:

$$D = (B - A) + C \tag{B.1}$$

This transformation keeps the total vessel mass unchanged, but updates the centre of gravity and rotational inertias because the legs are moved from the raised to the lowered position.

For each configuration, the rigid-body mass matrix is written as

$$\mathbf{M}_i = \begin{bmatrix} m_i & 0 & 0 & 0 & 0 & 0 \\ 0 & m_i & 0 & 0 & 0 & 0 \\ 0 & 0 & m_i & 0 & 0 & 0 \\ 0 & 0 & 0 & I_{x,i} & 0 & 0 \\ 0 & 0 & 0 & 0 & I_{y,i} & 0 \\ 0 & 0 & 0 & 0 & 0 & I_{z,i} \end{bmatrix}, \qquad i \in \{A, B, C, D\} \tag{B.2}$$

where m_i is the mass and $I_{x,i}$, $I_{y,i}$, and $I_{z,i}$ are the rotational inertias about the centre of gravity of configuration i. The centre of gravity is given by

$$\mathbf{r}_{CG,i} = \begin{bmatrix} x_{CG,i} \\ y_{CG,i} \\ z_{CG,i} \end{bmatrix}. \tag{B.3}$$

The centre of gravity of the resulting legs-down configuration is calculated by mass-weighted addition and subtraction:

$$m_E \mathbf{r}_{CG,E} = m_B \mathbf{r}_{CG,B} - m_A \mathbf{r}_{CG,A} + m_C \mathbf{r}_{CG,C} \tag{B.4}$$

with

$$m_E = m_B - m_A + m_C. \tag{B.5}$$

The rotational inertias are not added and subtracted directly about their own centres of gravity. Instead, all inertia terms are first shifted to a common reference point using the parallel-axis theorem.

For the inertia calculation, the contributions of Situations A, B and C are combined using the parallel-axis theorem. The inertia tensor of the legs-down configuration about its own centre of gravity is obtained directly as

$$\begin{aligned} \mathbf{I}_{CG,E} = &\left[\mathbf{I}_{CG,B} + m_B \left(\left(\mathbf{d}_{B,E}^T \mathbf{d}_{B,E}\right) \mathbf{I}_3 - \mathbf{d}_{B,E} \mathbf{d}_{B,E}^T\right)\right] \\ &- \left[\mathbf{I}_{CG,A} + m_A \left(\left(\mathbf{d}_{A,E}^T \mathbf{d}_{A,E}\right) \mathbf{I}_3 - \mathbf{d}_{A,E} \mathbf{d}_{A,E}^T\right)\right] \\ &+ \left[\mathbf{I}_{CG,C} + m_C \left(\left(\mathbf{d}_{C,E}^T \mathbf{d}_{C,E}\right) \mathbf{I}_3 - \mathbf{d}_{C,E} \mathbf{d}_{C,E}^T\right)\right], \end{aligned} \tag{B.6}$$

where

$$\mathbf{d}_{i,E} = \mathbf{r}_{CG,i} - \mathbf{r}_{CG,E}, \qquad i \in \{A, B, C\}. \tag{B.7}$$

Here, $\mathbf{I}_{CG,i}$ is the inertia tensor of configuration i about its own centre of gravity, m_i is the corresponding mass, $\mathbf{r}_{CG,i}$ is the centre-of-gravity position, and $\mathbf{I}_3$ is the 3×3 identity matrix. The minus sign for Situation A represents the removal of the legs-up contribution, while the plus sign for Situation C represents the addition of the legs-down contribution.

The final mass matrix used for the impact simulations is therefore

$$\mathbf{M}_E = \begin{bmatrix} m_E & 0 & 0 & 0 & 0 & 0 \\ 0 & m_E & 0 & 0 & 0 & 0 \\ 0 & 0 & m_E & 0 & 0 & 0 \\ 0 & 0 & 0 & I_{x,E} & 0 & 0 \\ 0 & 0 & 0 & 0 & I_{y,E} & 0 \\ 0 & 0 & 0 & 0 & 0 & I_{z,E} \end{bmatrix}. \tag{B.8}$$

C Derivation for strain energy in legs

Start from

$$E_{\text{strain}} = \int_0^L \frac{M(x)^2}{2EI}\, dx. \tag{C.1}$$

For a clamped–free beam with end load F,

$$M(x) = F(L - x). \tag{C.2}$$

Substitute:

$$E_{\text{strain}} = \int_0^L \frac{F^2(L-x)^2}{2EI}\, dx. \tag{C.3}$$

Factor constants:

$$E_{\text{strain}} = \frac{F^2}{2EI} \int_0^L (L-x)^2\, dx. \tag{C.4}$$

Integrate:

$$\int_0^L (L-x)^2\, dx = \left[\frac{(L-x)^3}{-3}\right]_0^L = \frac{L^3}{3}. \tag{C.5}$$

Result:

$$E_{\text{strain}} = \frac{F^2 L^3}{6EI}. \tag{C.6}$$

At the clamp:

$$M_{LH} = FL. \tag{C.7}$$

Substitute $F = M_{LH}/L$:

$$E_{\text{strain}} = \frac{M_{LH}^2 L}{6EI}. \tag{C.8}$$

For two directions:

$$E_{\text{strain},x} = \frac{M_{LH,x}^2 L}{6EI_x}, \qquad E_{\text{strain},y} = \frac{M_{LH,y}^2 L}{6EI_y}. \tag{C.9}$$

Total:

$$E_{\text{strain}} = E_{\text{strain},x} + E_{\text{strain},y}. \tag{C.10}$$

Free-floating 3hr energy response of allowable cases D

This appendix presents the time-dependent energy results for the 34 allowable cases considered in the case-variation study. The results are shown on the next page due to space limitations.


Batch 4 - Tp = 10 s
Etot
Ek
Ep
Case 000 | Dir 0 | seed 0
Case 005 | Dir 30 | seed 0
Case 010 | Dir 60 | seed 0
Case 015 | Dir 90 | seed 0
Case 020 | Dir 120 | seed 0
Case 025 | Dir 150 | seed 0
Case 030 | Dir 180 | seed 0
1e8
Energy [J]
0.0
0.5
1.0
1.5
2.0
2.5
0
2000
4000
6000
8000
10000
Time [s]

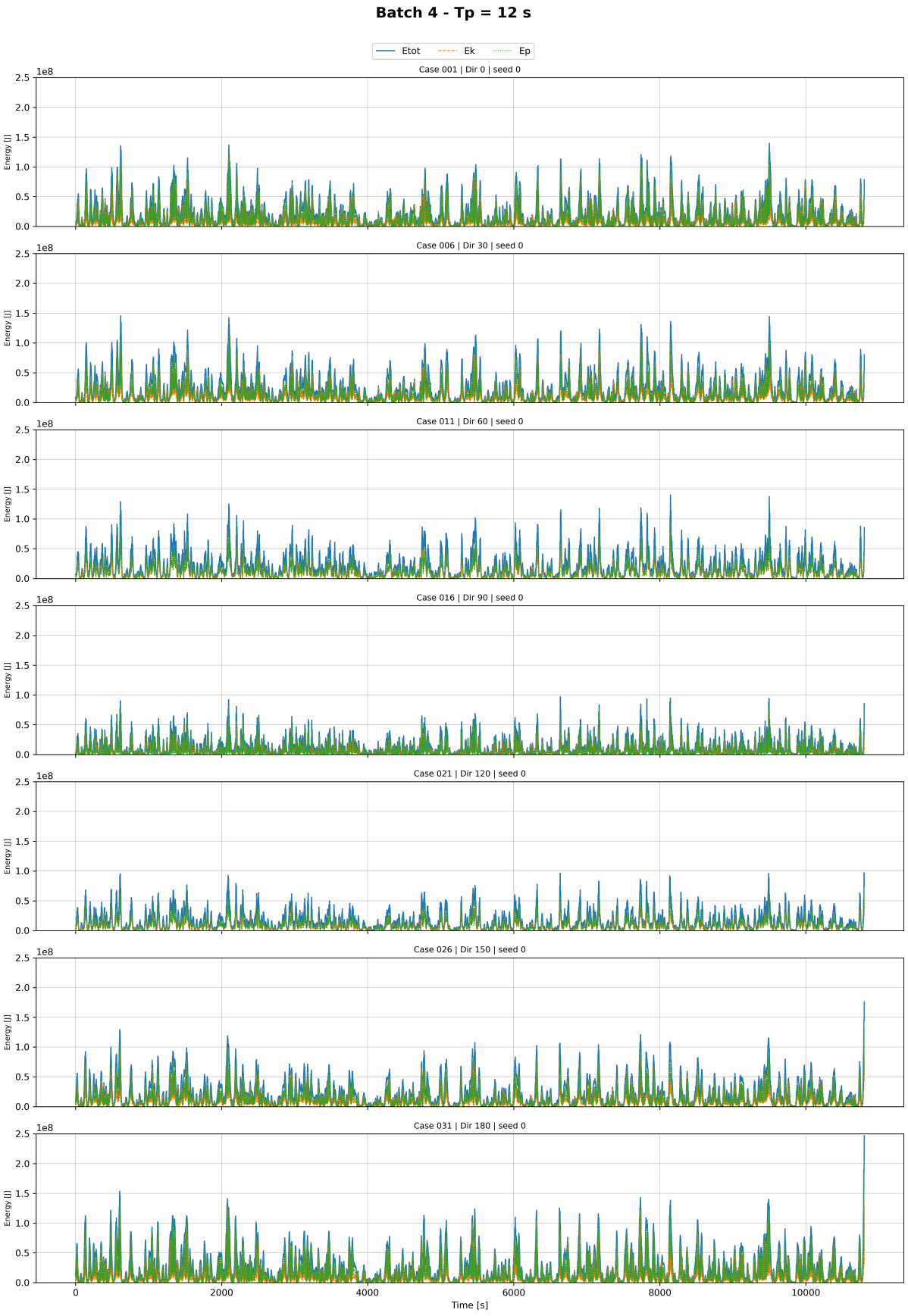
Batch 4 - Tp = 12 s
Etot
Ek
Ep
Case 001 | Dir 0 | seed 0
Case 006 | Dir 30 | seed 0
Case 011 | Dir 60 | seed 0
Case 016 | Dir 90 | seed 0
Case 021 | Dir 120 | seed 0
Case 026 | Dir 150 | seed 0
Case 031 | Dir 180 | seed 0
1e8
Energy [J]
0.0
0.5
1.0
1.5
2.0
2.5
0
2000
4000
6000
8000
10000
Time [s]

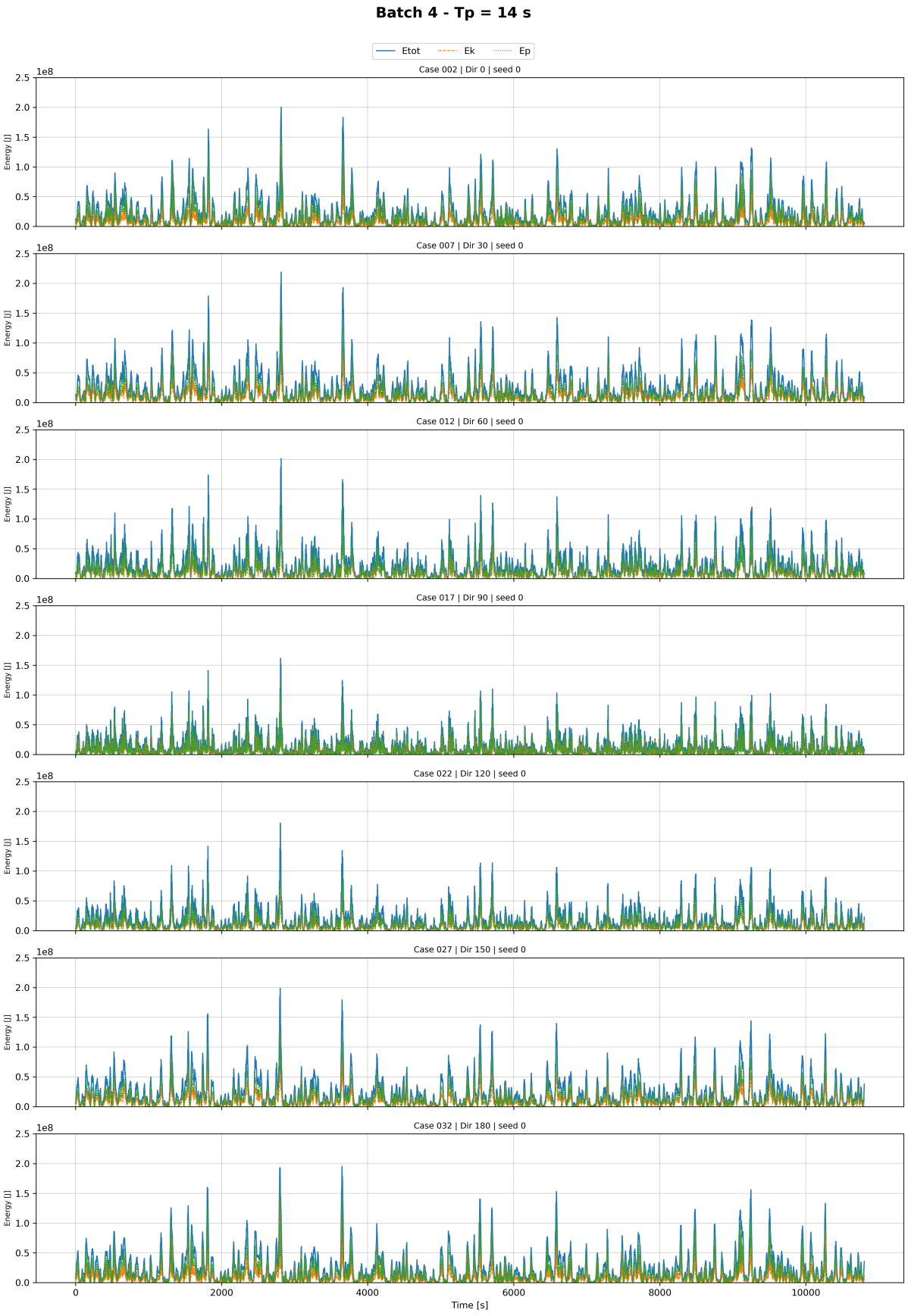
Batch 4 - Tp = 14 s
Etot
Ek
Ep
Case 002 | Dir 0 | seed 0
Case 007 | Dir 30 | seed 0
Case 012 | Dir 60 | seed 0
Case 017 | Dir 90 | seed 0
Case 022 | Dir 120 | seed 0
Case 027 | Dir 150 | seed 0
Case 032 | Dir 180 | seed 0
1e8
Energy [J]
0.0
0.5
1.0
1.5
2.0
2.5
0
2000
4000
6000
8000
10000
Time [s]

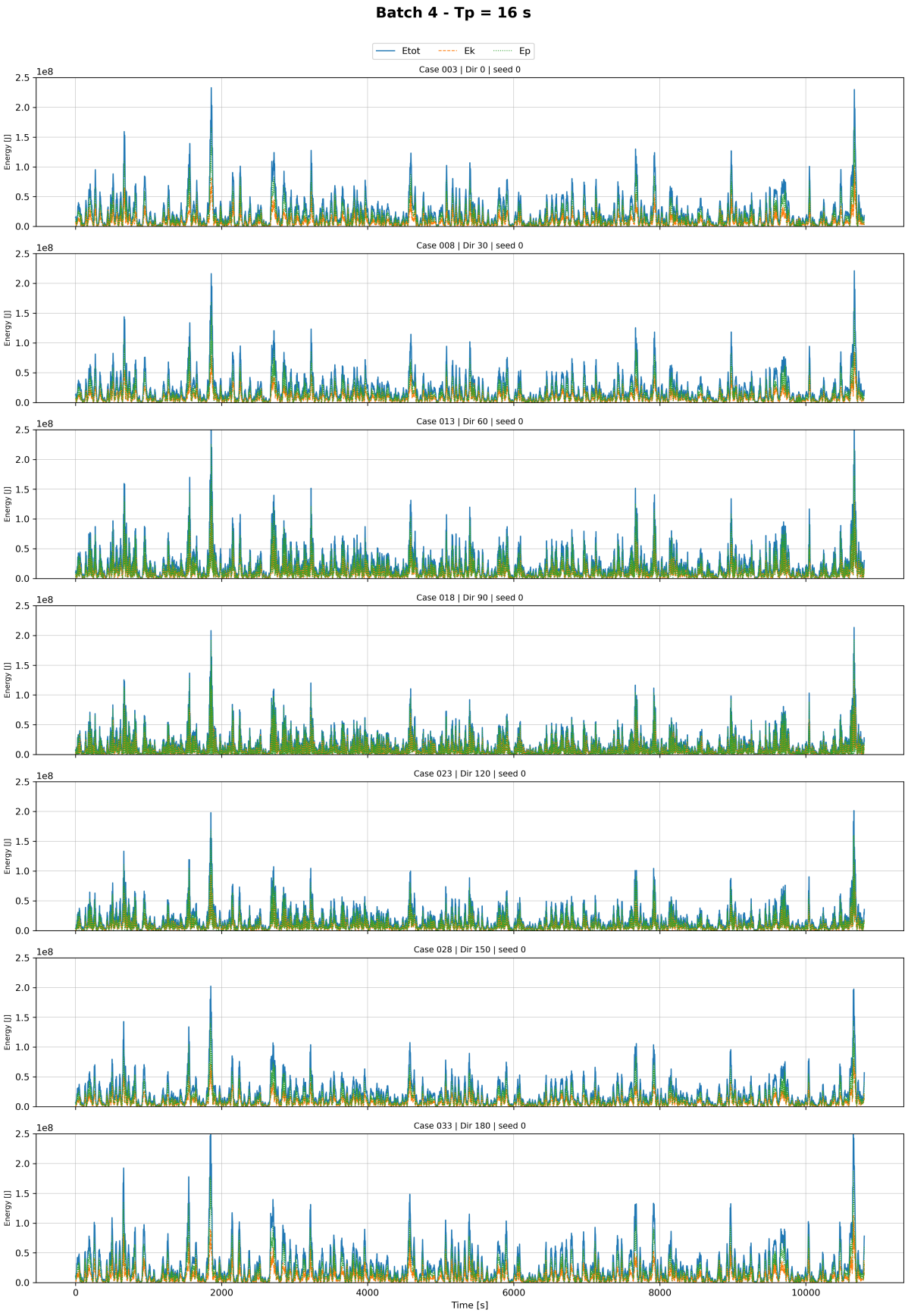
Batch 4 - Tp = 16 s
Etot
Ek
Ep
Case 003 | Dir 0 | seed 0
Case 008 | Dir 30 | seed 0
Case 013 | Dir 60 | seed 0
Case 018 | Dir 90 | seed 0
Case 023 | Dir 120 | seed 0
Case 028 | Dir 150 | seed 0
Case 033 | Dir 180 | seed 0
1e8
Energy [J]
0.0
0.5
1.0
1.5
2.0
2.5
0
2000
4000
6000
8000
10000
Time [s]

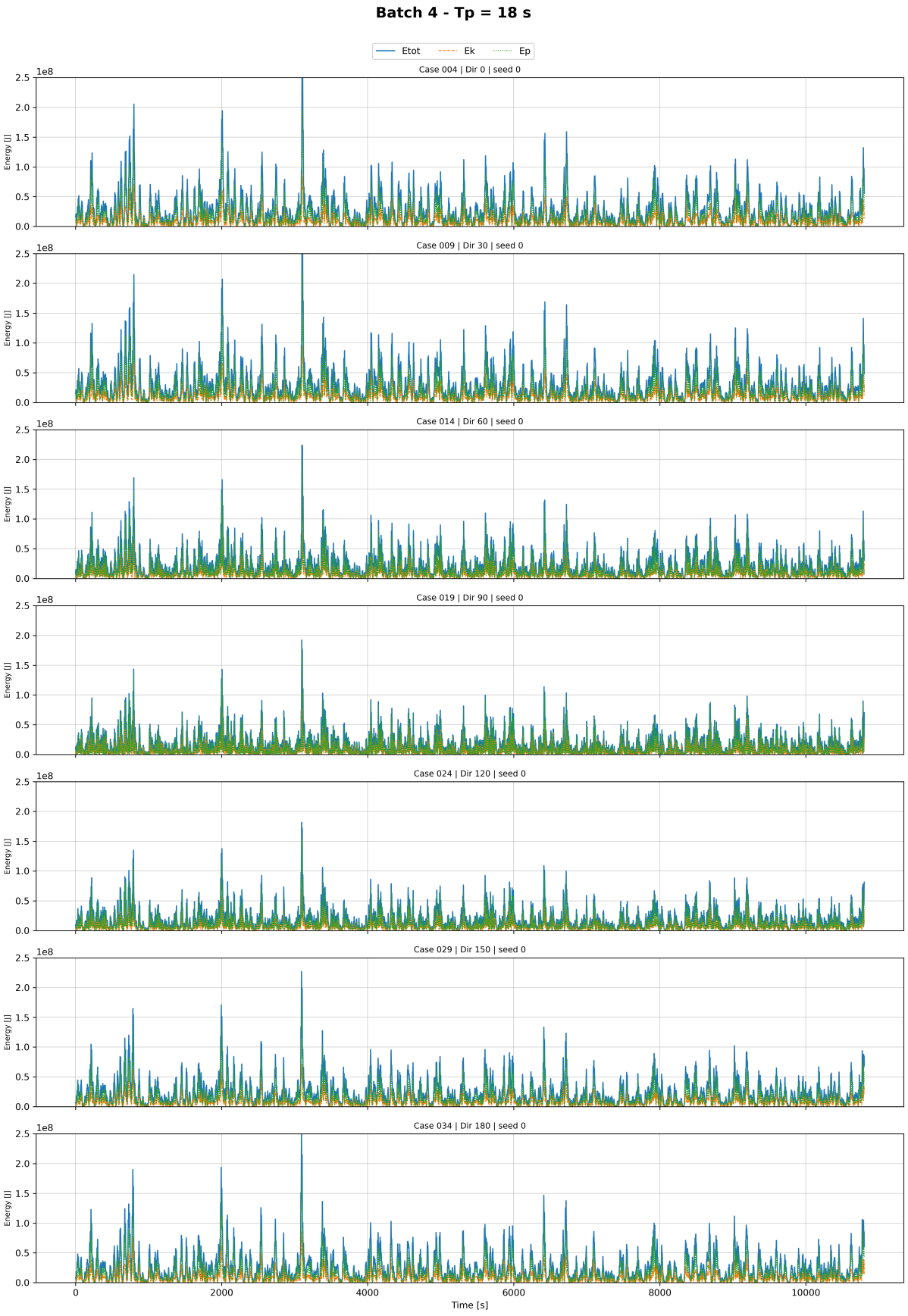
Batch 4 - Tp = 18 s
Etot
Ek
Ep
Case 004 | Dir 0 | seed 0
Case 009 | Dir 30 | seed 0
Case 014 | Dir 60 | seed 0
Case 019 | Dir 90 | seed 0
Case 024 | Dir 120 | seed 0
Case 029 | Dir 150 | seed 0
Case 034 | Dir 180 | seed 0
1e8
Energy [J]
0.0
0.5
1.0
1.5
2.0
2.5
0
2000
4000
6000
8000
10000
Time [s]